

**EXPERIMENTATION ON MULTI-WIRES
ELECTROCHEMICAL MACHINING (MWECEM)
FOR FABRICATION OF MICRO FEATURES**

By

Sovan Maity

EXAMINATION ROLL NO. – M4PRD19007

THESIS

SUBMITTED IN PARTIAL FULFILMENT OF THE REQUIREMENTS FOR THE
AWARD OF THE DEGREE OF MASTER OF ENGINEERING IN PRODUCTION
ENGINEERING IN THE FACULTY OF ENGINEERING & TECHNOLOGY OF
JADAVPUR UNIVERSITY

**DEPARTMENT OF PRODUCTION ENGINEERING
JADAVPUR UNIVERSITY
KOLKATA-700 032
INDIA
2019**

JADAVPUR UNIVERSITY
FACULTY OF ENGINEERING AND TECHNOLOGY

CERTIFICATE OF RECOMMENDATION

I/WE HEREBY RECOMMEND THAT THE THESIS ENTITLED
“**EXPERIMENTATION ON MULTI-WIRES ELECTROCHEMICAL
MACHINING (MWECM) FOR FABRICATION OF MICRO FEATURES**”
CARRIED OUT UNDER MY/OUR SUPERVISION AND GUIDANCE, BY **SRI
SOVAN MAITY**, MAY BE ACCEPTED IN THE PARTIAL FULFILLMENT OF THE
REQUIREMENTS FOR THE DEGREE OF “**MASTER OF ENGINEERING IN
PRODUCTION ENGINEERING**”.

Countersigned

Thesis Advisor

HEAD
(Dr. Biplab Ranjan Sarkar)
Associate Professor,
Dept. of Production Engineering,
JADAVPUR UNIVERSITY,
Kolkata – 700 032.

(Dr. Bijoy Bhattacharyya)
Professor,
Dept. of Production Engineering,
JADAVPUR UNIVERSITY,
Kolkata – 700 032.

DEAN,
Faculty of Engineering and Technology,
JADAVPUR UNIVERSITY,
Kolkata – 700 032

JADAVPUR UNIVERSITY
FACULTY OF ENGINEERING AND TECHNOLOGY

CERTIFICATE OF APPROVAL*

The foregoing thesis is hereby approved as a creditable study of an engineering subject carried out and presented in a manner of satisfactory to warrant its acceptance as a pre-requisite to the degree for which it has been submitted. It is understood that by this approval, the undersigned do not necessarily endorse or approve any statement made, opinion expressed and conclusion drawn therein but approve the thesis only for the purpose for which it has been submitted.

**COMMITTEE ON
FINAL EXAMINATION
FOR EVALUATION OF
THE THESIS**

(External Examiner)

(Internal Examiner)

* Only in case the recommendation is concurred in

ACKNOWLEDGEMENT

It is my greatest fortune to perform the thesis work in the Production Engineering Department, Jadavpur University.

It is a great pleasure to express my gratitude and indebtedness to my esteemed guide Dr. B. Bhattacharyya, Professor, Department of Production Engineering, Jadavpur University. It is because of his noble and continuous guidance, encouragement as well as valuable advices at every aspect and strata of the problem from the embryonic to the development stage that my thesis has been in the light of the day.

My special thanks to Head of Production Engineering Department for allowing me to carry out the research investigation with various facilities of the department. I would like to express my warmest gratitude to all respected teachers of this department who took keen interest in the work and helped me with valuable suggestions.

I am thankful to Science and Engineering Research Board (SERB), DST, New Delhi, for the financial assistantship to carry out the research work. I also want to express my heartiest thanks to Mr. Subhrajit Debnath, senior research fellow (SRF) under SERB, DST sponsored project, as this research work and investigation is a joint effort of both of us.

The brawny support author has received from Mr. Koushik Mishra, senior research fellow (SRF) along with his valuable support as well as suggestions are beyond the acknowledgement.

Appreciation is also due to Mr. Santosh Kumar, Mr. Raju M. Tayade, Mr. Nilanjan Roy, Mr. Subrata Mahata, Mr. Sandip Kunar and all other research scholars for their constant co-operation, useful assistance and support during this research work. I also appreciate the support of librarians, technicians especially Mr. Biswajit Pathak and other staffs of our department for their cordial assistance throughout my thesis work. I express my appreciation to my friends for their understanding, patience and active co-operation throughout my M. Prod. E. course.

Last but not the least, I would like to thank my parents for their endless support, guidance and sacrifice for my education, and all the family members for their constant encouragement in the pursuit of this research work.

(SOVAN MAITY)

Examination Roll No.: M4PRD19007

TABLE OF CONTENTS

	Page No
TITLE SHEET	i
CERTIFICATE OF RECOMMENDATION	ii
CERTIFICATE OF APPROVAL	iii
ACKNOWLEDGEMENT	iv
TABLE OF CONTENTS	v
Chapter 1	
1 Introduction	
1.1 Advancement of Electrochemical Micromachining (EMM) process	1
1.2 Concept of Wire Electrochemical Machining (WECM)	1-2
1.3 Advancement of Wire Electrochemical Machining (WECM)	2
1.4 Literature survey of past research works	3-15
1.5 Objectives and scope of present research	15-16
Chapter 2	
2 Fundamentals of Multi-wire Electrochemical Machining (MWECEM)	
2.1 Principle of Multi-wire Electrochemical Micromachining	17-19
2.2 Different machining conditions in Multi-wire Electrochemical Micromachining	19-20
2.3 Equivalent Circuit for Multi-wire Electrochemical Machining	20-21
2.4 Advantages of Multi-wire Electrochemical Machining	22
2.5 Application of Multi-wire Electrochemical Machining	22-23
Chapter 3	
3 Development of Multi-wire electrochemical machining (MWECEM) experimental setup	
3.1 Various developed components of MWECEM	24-25
3.1.1 Multi-wires holding device	
3.1.2 Machining chamber	
3.2. Various sub-systems of MWECEM set-up	26-29
3.2.1 XYZ movement stage	
3.2.2 Power supply unit	
3.2.3 Vibration unit	
3.2.4 Ancillary unit	

Chapter 4

- 4 Development of mathematical modelling for multi-wires electrochemical micromachining
- 4.1 Correlation of the process parameters with the width of the micro slit 30-36

Chapter 5

- 5 Experimentation on Multi-wire Electrochemical Machining
- 5.1 Preliminary Experimentation in MWECEM 37-39
 - 5.1.1 Planning for Preliminary experimentation
 - 5.1.2 Results and discussions
- 5.2 Axial flushing assisted MWECEM 39-46
 - 5.2.1 Planning for experimentation
 - 5.2.2 Results and discussions
- 5.3 Vibration assisted MWECEM 46-53
 - 5.3.1 Planning for experimentation
 - 5.3.2 Results and discussion
- 5.4 Combination of axial flushing and vibration assisted MWECEM 53-57
 - 5.4.1 Planning for experimentation
 - 5.4.2 Results and discussion
- 5.5 Comparison among different flushing criteria incorporated with MWECEM 57-59
- 5.6 Analysis and validation of mathematical model of slit width 59-61
- 5.7 Fabrication of micro features using Multi-wire Electrochemical Machining process 61-62

Chapter 6

- 6 General conclusions 63-65

References

66-68

1. INTRODUCTION

1.1 Advancement of Electrochemical Micromachining (EMM) process

Electrochemical machining (ECM) is based on Faraday's law of electrolysis which is an anodic dissolution process. In ECM, the work piece acts as an anode and the tool as the cathode, and they are separated by a small gap in an electrolytic cell. When a DC pulse is applied through the electrolyte, the anode work piece dissolves locally so that the shape of the generated work piece is approximately a complimentary shape of the tool. When ECM is applied for micromachining, it is called EMM (Electrochemical Micro Machining). EMM has ability of machining complex shapes and chemically resistant metals, e.g., super alloys, titanium, and copper alloys, and high flexibility and environment friendliness. EMM which is based on electrochemical dissolution, appears to be a very promising method for shaping these materials because of its ability to produce a good surface finish without generating a heat-affected zone or residual stresses in the workpiece, together with the absence of tool wear and an independence of material hardness and melting point. EMM appears to be a very promising micromachining technology due to its advantages that include high machining rate, better precision and control, rapid machining time, reliability, flexibility, and being environmentally acceptable, and also because it permits machining of chemically resistant materials like titanium, copper alloys, super alloys, and stainless steel, which are widely used in biomedical, electronic and MEMS applications. Since the anode material dissolves electrochemically, its rate of machining depends only upon the atomic weight (A) and valency (z) of the ions produced, the current (I) that is passed, and the time (t) for which the current passes. The hardness, toughness, and thermal resistance do not influence the MRR. Using the EMM techniques generates more freedom in designing a microproduct. High dimensional accuracy and high surface quality can be achieved with this process.

1.2 Concept of Wire Electrochemical Machining (WECM)

In Wire Electrochemical Machining (WECM), the material removal takes place by electrochemical reactions between suitable dimensional wire which is made cathode and the workpiece which is made anode. Here the wire tool is fed towards the workpiece

to start the anodic dissolution process and is moved within the workpiece in a predetermined path to fabricate microfeatures with desired profile. This WECM process is relatively new and extensive amount of research is still needed on different aspects to make this process efficient and industry ready.

wire electrochemical micro-machining (WECM), a special type of EMM, has come to be recognized as a flexible method for the fabrication of complex-shaped planar microstructures. It not only possesses the basic advantages of EMM, but also does not require the fabrication of a complex-shaped cathode. WECM is superior to wire electric discharge micromachining in that it neither suffers from surface defects nor wears out tool electrode. Thus, a thinner wire can be repeatedly used in WECM.

However, during machining, ongoing electrochemical reactions result in the formation of sludge and hydrogen bubbles. These machining products may stick between the tool and the work piece which can clog the small IEG resulting in formation of micro sparks and deterioration of machining quality and accuracy. Therefore, to remove the electrolysis products from the IEG and to supply fresh electrolytes, various means such as application of piezoelectric transducer (PZT), use of reciprocating travelling wire, utilization of axial electrolyte flow etc. are adopted.

1.3 Advancement of Wire Electrochemical Machining (WECM)

Although there have been many investigations of WECM, these are experiment with ribbed wire in WECM, anode vibration assisted WECM process, intermediate feed directional motion of wire which make flushing in WECM process etc., its application in industry is still limited because of its relative low machining efficiency. A method namely Multi-wires electrochemical machining (MWECM) had been proposed to increase the productivity in machining arrayed structures which is the next level of advancement in WECM. MWECM employs an array of metallic wires as the cathode, thus an array of microstructures could be machined simultaneously. WECM using multi-wire electrodes, in which multiple features of the same shape are fabricated in one process, is a perfect method to improve machining efficiency. In this way multi-wire electrochemical micromachining will play an important role to improve the machining productivity of WECM.

1.5 Literature survey of past research works

Zeng et al. [1] presented three mass transport enhancing approaches namely, electrolyte flushing along the wire, ring wire travelling in one direction and micro-vibration of cathode wire for renewing the electrolyte in the machining gap. In their study the authors considered the fact that the composition and concentration of the electrolyte in the gap would be changed by electrolysis product. The electrolyte flow with 0° entrance angle was suggested in this study in case of electrolyte flushing and the optimal electrolyte flowrate and wire feedrate was determined to be 0.75 m/s and 0.5 $\mu\text{m/s}$, respectively. In case of the wire travelling in one direction, the direction was arranged to be always in coincident with the direction of gravity. The optimal wire travelling speed was 0.015 m/s and with the optimal wire travelling speed, the wire feedrate could reach up to 1.0 $\mu\text{m/s}$. Low frequency and small amplitude vibration of cathode wire was induced by a piezo-electric transducer (PZT) and the direction of the micro vibration was arranged to always parallel to the wire electrode axis. The finest machining stability could be obtained with wire vibration frequency of 10 Hz and amplitude of 8 μm . The authors found that with the electrolyte flushing, microstructures with the aspect ratio up to 30 could be obtained. Wire travelling was capable of producing microstructures having feature heights up to 10 μm and feature aspect ratios of 50 or more. However, thick wire was used for avoiding wire breakage and direct current was used as the power of the ultra-short voltage pulses was not enough. For fabricating microstructures with high precision features, micro-vibration of cathode wire was suggested because thin wire of diameter less than 10 μm could be used.

Xu et al. [2] adopted enhancement methods of mass transport, namely anode vibration at low frequencies and cathode travelling in the axial direction of the cathode, to decrease surface roughness when using wire electrochemical micro machining (WEMM). A tungsten wire, insulated with silastic except for the machining area, of 10 μm diameter was adopted as the cathode electrode. The workpiece was cobalt-based alloy of 80 μm thickness and the electrolyte was hydrochloric acid with a concentration of 0.01 M. In all the experiments the wire electrode feedrate was set at 0.2 $\mu\text{m/s}$. In this study it was found that the roughness of the machining surface was affected by mass transport conditions and the influence of cathode travelling and anode vibration parameters on the surface roughness were investigated. Optimal conditions revealed

from the experiments were a speed of $400 \mu\text{ms}^{-1}$ with amplitude of $100 \mu\text{m}$ for cathode travelling and a frequency of 5 Hz with amplitude of $100 \mu\text{m}$ for anode vibration. It was also found that the low voltage and short pulse duration reduced the electrolytic product, and the long period allowed more time for mass transport, which both led to a low dissolution rate. However, too low a dissolution rate caused short circuiting which resulted in high surface roughness. Therefore, an optimal pulse condition of 6 V voltage, 40 ns duration and $6 \mu\text{s}$ period was obtained. Surfaces with R_a value of $0.058 \mu\text{m}$ and R_{max} value of $0.670 \mu\text{m}$ were obtained using the optimal machining condition, and micro cams of external sizes $150 \mu\text{m}$ and $400 \mu\text{m}$ were fabricated on a cobalt-based super alloy.

Ningsong et al. [3] proposed wire electrochemical machining with axial electrolyte flushing for the fabrication of titanium alloy (TC1) sheet with 0.18 mm thickness in combined NaCl and NaNO_3 electrolyte solution. Taguchi experiment was carried out to determine the optimal combination level of the machining parameters which could achieve a smaller side gap under a stable machining process. The five independent parameters were electrolyte concentration, nozzle workpiece distance, electrolyte flowrate, working voltage, and wire feedrate, which were arranged as five levels in an $L_{25}(5^6)$ orthogonal Taguchi array. The optimal machining parameters found were $2.5\% \text{ NaCl} + 2.5\% \text{ NaNO}_3$, 5 mm nozzle-work piece distance, 87 m/s electrolyte flowrate, 18 V working voltage, and 1.8 mm/min wire federate. Furthermore, the complex structures were fabricated by multi-wire electrochemical machining with axial electrolyte flushing with 5 wires and wire feedrate was 0.6 mm/min .

Xu et al. [4] introduced WEMM as a fabrication technique of micro square column tool array and used electrode vibration to improve the machining accuracy, stability and feed rate. Simulations of the electric field were done to study the influences of bubble behaviour on the slit width homogeneity and edge radius. The results showed that the remaining bubble in the machining gap reduced the current density on the anode surface near the bubble than that on the other part of anode surface in the machining gap resulting in poor homogeneity of slit width and the remaining bubble near the edge of the workpiece increased the current density resulting in higher edge radius. When only anode vibration was applied, large particles of insoluble product are produced and accumulation of bubbles on the surface of the wire cathode could not be prevented. The

authors suggested large amplitudes and high speeds of cathode vibration, and large amplitudes and high frequencies of anode vibration to drive the bubbles out of the machining gap and prevent accumulation of insoluble product. Tungsten wire of diameter $10\mu\text{m}$ was used and the array micro tools were fabricated on cobalt-based alloy of thickness $80\mu\text{m}$ in dilute hydrochloric acid at a concentration of 0.05M . The experimental study revealed that pulses with low voltages, long periods and short durations and high feed rate improved the homogeneity of the slit width and reduced the edge radius. The optimal parameter settings were $200\mu\text{m}$ amplitude and $400\mu\text{m/s}$ speed for cathode vibration, $5\mu\text{m}$ amplitude and 100 Hz frequency for anode vibration, 5 V voltage, $6\mu\text{s}$ period and 50 ns duration for the pulse, 0.05M electrolyte concentration and $0.5\mu\text{m/s}$ feed rate. With this parameter settings micro beams were produced in first step and micro square columnar tool arrays were fabricated in second step. Each micro tool was $140\mu\text{m}$ long with a section size of $10 \times 10\ \mu\text{m}^2$. When multi wires were used to fabricate the array tool electrode, the electrical parameters were adjusted to 6 V for voltage, $5\ \mu\text{s}$ for period and 90 ns for duration because the process demanded more energy. Furthermore using the square column tool array, micro dimple array of depth of $15.9\ \mu\text{m}$ with entrance size of $25.5 \times 24.6\ \mu\text{m}$ were electrochemically fabricated.

Meng et al. [5] introduced WECMM for processing of Ni-based metallic glass ($\text{Ni}_{72}\text{Cr}_{19}\text{Si}_7\text{B}_2$) in dilute hydrochloric acid electrolyte. Simulation study of the electric field in the machining gap was done to study the bubbles behaviour and the distorted contours of electric field lines showed that the bubbles significantly influenced the current density distribution which led to a lack of homogeneity of the machined slit. The cathode wire travelling and anode workpiece vibration technique was suggested as an effective method to enhance mass transport and maintain a stable machining current density. Experiments were conducted on metallic glass $\text{Ni}_{72}\text{Cr}_{19}\text{Si}_7\text{B}_2$ with a thickness of $50\ \mu\text{m}$ with a $10\ \mu\text{m}$ -diameter tungsten wire and electrolyte was prepared from de-ionized water and analytical grade HCl (37%). The polarization behaviour was studied from the polarization curve of the Ni-based glassy alloy in 0.1 M HCl and it was characterized by active dissolution, passivation and transpassivation zones. Ni and Cr both affected the passivation reaction and the increased current density indicated that the passive film was broken down by the adsorptive action of chlorine ions. The surface topography of the Ni- based glassy alloy after processing was significantly non-uniform

but it was improved by optimizing the machining parameters. It was found from the experimental results that a the side gap, obtained at short pulse duration with low feed rate, was smaller than that obtained at long pulse duration with high feed rate. For stable and efficient machining, the optimal parameter setting found was HCl electrolyte concentration of 0.1M, applied voltage of 4.5 V, pulse duration of 80 ns, pulse period of 3 μ s, and feed rate of 0.3 μ m/s. Several complex microstructures such as micro curved channel with an average slit width of 14.2 μ m and standard deviation of 0.25 μ m, micro square helix with an average slit width of 14.0 μ m and standard deviation of 0.2 μ m, micro gear with an average slit width of a tooth of 14.5 μ m and a standard deviation of 0.3 μ m and a pentagram structure with a side length of 90 μ m and sharp corner of 36° were fabricated.

He et al. [6] proposed a method of WECMM using axial vibration-assisted multi-wire electrodes with high travelling speed and a flow-field model was established to simulate the flow field in the machining gap when the travelling wire electrode was used. Simulation results revealed that greater mass transport efficiency was feasible at higher tool travel speeds. 50 μ m diameter tungsten wires were fixed into the tool fixture at intervals of 1.0 mm and the tension was 5N. Stainless steel (304) with the thickness of 3 mm was employed as anode and the electrolyte was 0.06M NaNO₃. Experiments were done to study the effects of the parameters on the machining accuracy and efficiency. The experimental results showed that a higher feed rate could be applied when there were fewer electrodes because of the higher MRR and the greater mass transport efficiency. Using vibration amplitude of 10 mm, a pulse voltage of 18 V, a pulse frequency of 50 kHz, and a pulse duty cycle of 35%, the maximum feed rate achieved using 15-wire electrodes was 5.0 μ m/s and the total machining rate was 75 μ m/s, which was ten times that of using single wire in WECMM. A multiple-slit microstructure with aspect ratio of 20 was produced with insignificant taper and good consistency. Furthermore, the authors mass-produced X-shaped microparts of high quality ($R_a = 128.0$ nm, $R_q = 162.0$ nm, and $R_{max} = 1.72$ μ m) at a total machining rate of 35.0 μ m/s using 7-wire electrodes.

Xiaolong et al. [7] proposed a method for WECMM using a rotary helical electrode and studied the effect of the rotary helical electrode on the flow field by simulation, and a series of experiments was conducted to verify the simulation. The electrolyte in the

machining gap was stirred with the rotation of the electrode and the electrolysis products were diffused under forced convection driven by flow. It was proved that the axial velocity component of the electrolyte was the main reason for electrolyte refreshment in the machining gap and electrode rotation was helpful for enhancing process stability in WECMM. Simulation results indicated that a rotary helical electrode helped in generation of an axial velocity which in turn dragged the electrolyte flow from the bottom upwards. As the bubbles escaped upwards from the machining zone under the action of buoyancy, the authors suggested the clockwise direction of spindle rotation so that the machining products could flush out in the same direction. The experiments were conducted on the stainless steel 304 samples with dimensions of 20 mm×4 mm×4 mm in 20 g/L NaNO₃ electrolytic solution and initial interelectrode gap of 0.1 mm in the feeding direction was set. When the simple cylindrical electrode was used maximum feed rate was 2 μm/s with 5000 rpm and when the spindle speed was 20000 rpm, the improved to 6 μm/s. But slit width error in depth direction also increased from 10 μm to 20 μm. When a helical electrode was employed, the electrode feed rate remained at 4 μm/s for the spindle speed range of 500–8000 rpm and when the speed was 50000 rpm, the maximum feed rate achieved was 7 μm/s, which was eight times that of the feed rate using a static cylindrical electrode. Employment of helical electrode reduced the slitwidth error to 5 μm. Furthermore, complex structures such as a fir-tree-like structure with a thickness of 3 mm and a space hollow structure on a substrate with dimensions of 3mm×3mm were fabricated with electrode feed rate of 6 μm/s and the spindle speed of 20000 rpm.

He et al. [8] investigated the process for the WECMM of pure tungsten with a low electrolyte concentration and a small pulse duration. The influences of some of the key parameters such as feed rate, pulse duration, electrolyte concentration, applied voltage and pulse period on the side gap were studied. A commercial 10 μm-diameter tungsten wire was employed as the cathode and a KOH solution was employed as the electrolyte. Alkaline electrolyte was preferred because during electrochemical reaction of pure tungsten, WO₃ anodic film, which did not dissolve in acidic and neutral solutions, formed on the machined surface, and prevented the subsequent electrochemical dissolution. A vibration unit (PZT) was employed to vibrate the workpiece at low frequency and wire electrode was reciprocated along its axis for the renewal of electrolyte. The results revealed that a smaller side gap was obtained at small pulse

duration with low feed rate, compared to the use of large pulse duration with high feed rate and the edge of the machined slit at small pulse duration was smoother and more uniform than that at large pulse duration. In order to achieve a small side gap and a stable process the optimum combination of process parameters was found to be feed rate of 0.1 $\mu\text{m/s}$, KOH electrolyte concentration of 0.1 mol, applied voltage of 5 V, pulse period of 0.6 μs and pulse duration of 60 ns. With this combination the authors fabricated microstructures with a side gap of 4 μm , slit width of 18 μm and aspect ratio of 5.6 in 100 μm thick tungsten substrate. Applying a pulse period of 0.9 μs and pulse duration of 90 ns, microstructures with a side gap of 5 μm , slit width of 20 μm and aspect ratio of 15 was also produced in 300 μm thick substrate. Furthermore, preliminary tests of multiwire electrochemical micro machining of pure tungsten were studied and using a 3-wire electrode, a 9-slit microstructure with a slit width of 24 μm was produced and the machining efficiency was improved by a factor of three.

Zeng et al. [9] identified the characteristics of the stray-current attack in reciprocated travelling wire electrochemical machining and proposed special insulating methods to reduce the effect of the stray-current. The study revealed that the electrolysis products accumulated on the workpiece surface had positive effects on reduction of the stray-current attack and the stray-current attack was significantly affected by the wire traveling direction. The upper surface of the workpiece suffered the most serious stray-current attack, namely pitting corrosion, when the wire was traveling downward. To reduce the effect of stray-current caused by the wire electrode and the pulleys on the workpiece surface, the use of insulating tubes assisted with the shielding box was proposed in this study. The insulating tubes made of glass were closed to both sides of the workpiece surfaces and they were hollow inside to allow the wire electrode to pass through. The pulleys, used as the guide for the traveling wire electrode, were fixed in the shielding box. The simulation results revealed that the closer was the distance between the insulating tube and the workpiece, and the smaller was the tube inner diameter, the less stray-current attack would appear on the workpiece surface. The experiments were conducted on 20 mm thick SS 304 sheet with glass tube of 0.35 mm inner diameter and the distance of 0.05 mm between the insulating tube and the workpiece to verify the applicability of the proposed insulating methods. The cathode used was molybdenum wire of 100 μm diameter and the electrolyte used was 5g/L

NaNO₃ solution in 30°C. The authors fabricated complex structures with fine surface qualities when the insulation method was applied.

Xu et al. [10] discussed the effects of wire cathode surface hydrophilia on WEMM. A simplified flow formation model was developed with Couette motion and the transient flow was considered theoretically to show the influence of travelling wire and wire surface hydrophilia on electrolyte flow in machining gap. The analysis revealed that the high surface hydrophilia created a thick boundary layer and within the boundary layer, a large electrolyte viscosity, which enhanced mass transport when the reciprocating travelling wire method was used. Chemical etching, done by 0.5M KOH, was used to prepare a 10 µm diameter tungsten wire cathode with a good hydrophilic surface. During the wire fabrication process etching occurred in the intergranular area first and as time increased, other areas on the wire surface were dissolved producing a rough surface. The experimental study was done on the cobalt based alloy of thickness 80 µm and the electrolyte was dilute hydrochloric acid at a concentration of 0.01 M. The results revealed that the wire cathode with a rough surface improved machining stability and stable feed rate up to 0.45µm/s was achieved. The homogeneity of the micro slits including the homogeneity of each micro slit and the homogeneity between different micro slits was also improved by using a wire cathode with a rough surface. Moreover, the roughness average and maximum roughness depth values were lower than those when using a wire cathode with a smooth surface, confirming that the machined surface was smoother when using the wire cathode with a rough surface and when the feed rate was low enough to prevent taking place electrical short circuits or wire cathode deformation, a large feed rate led to a small roughness of the machined surface.

Qu et al. [11] introduced the combined method of vibrating anode with low frequency and travelling cathode in the axial direction of the cathode to improve the homogeneity of micro slits in wire electrochemical micro machining (WEMM). The vibration of the anode workpiece was given by a piezoelectric ceramics (PZT) unit. The experiments were conducted with tungsten wire of 4 µm diameter on a cobalt-based alloy with thickness of 80 µm in dilute hydrochloric acid with a concentration of 0.05 M and the constant wire electrode feedrate was 0.2 µm/s. The authors observed that the frequency of 100 Hz with amplitude of 5 µm was optimal for anode vibration and the frequency of 2 Hz with amplitude of 70 µm was optimal for electrode travelling. Moreover, it was

found that the applied voltage and the pulse duration significantly influenced the side gap width in WEMM. Low applied voltage and short pulse duration led to a narrow side gap. Using optimal parameters, the authors fabricated a group of slits and beams and cantilever curved beams with width of approximately 5 μm and aspect ratio of approximately 15.

Xu et al. [12] introduced multiple tungsten wire electrodes with diameters of 10 μm to improve the machining efficiency for fabricating micro structures with high-precision features and studied the effects of the number of wire electrodes on feed rate and overall efficiency. The electrolyte used was diluted hydrochloric acid of 0.01 M concentration and the workpiece was a cobalt-base elastic alloy with a thickness of 80 μm . It was revealed that when the same pulse on-time was applied, the feed rate decreased with increasing number of wire electrodes because with increasing the number of tool electrodes, the cell impedance decreased as the polarization resistance decreased and the double layer capacitance increased which in turn increased the rise time of the double layer potential and decreased the effective time for machining. The machining rate was determined as the multiplication of the number of electrodes and the feed rate. As the feed rate was not constant and decreased with increasing number of wire electrodes, the overall machining rate was not linearly varied to the number of wire electrodes. It was found from the experimental study that the maximum feed rates for one wire electrode and three wire electrodes were approximately 0.7 $\mu\text{m/s}$ and 0.45 $\mu\text{m/s}$, respectively and the overall machining rate of three wire electrode machining increased by nearly 100% of that of one wire electrode. Furthermore, the effects of the applied pulse voltage, pulse on-time, pulse period and feed rate on the uniformity of the slit widths were investigated and the optimal values were applied voltage of 6.0 V, pulse on-time of 40 ns, pulse period of 6 μs and feed rate of 0.2 $\mu\text{m/s}$. With these optimal machining parameters two complex tree shaped micro structures with slit width of 14.1 μm with a standard deviation of 0.05 μm and slit width of 14.4 μm with a standard deviation of 0.06 μm were fabricated.

Xiangyang et al. [13] investigated fabrication of micro annular grooves on surface of a aluminum alloy cylindrical rod of diameter 3 mm and length of 20 mm by WECMM. The dissolution characteristics of aluminum alloy in sodium nitrate solution were investigated. During the fabrication process the aluminium rod was rotated and moved

vertically and acted as anode. The tungsten wire electrode of 20 μm diameter acted as cathode and was moved perpendicular to the aluminum rod axis to fabricate the groove. An electrolyte nozzle was utilized for the refreshment of electrolyte and removal of electrolytic product from the machining zone. The measurement of anodic polarization curve was carried out by using a platinum net and a calomel electrode as the counter-electrode and reference electrode respectively. From the experiments it was revealed that aluminium hydroxide precipitated on the surface before it gradually changed to aluminum oxide forming the passive film and preventing the current flow and anodic dissolution process. When the anode potential was increased a steep increase of current density was observed due to the breakage of the passive film. However, it was also observed that the passive film, formed in non-machining zone, prevented the surface from stray corrosion due to low current density. Furthermore simulation was done to analyze of the current distribution between the rod workpiece and wire electrode. It was found that current density increased first with the overlap phase angle and then it decreased and as the wire electrode was fed towards the workpiece, the current density decreased in general. The effects of the machining parameters were analyzed and the optimal conditions were applied voltage of 9 V, pulse frequency of 150 kHz and the rod rotation speed of 2000 rpm. These conditions were employed to fabricate arrayed micro annular grooves with width of 100 μm , pitch of 80 μm and depth of 100 μm on the aluminium rod.

Xiaolong et al. [14] simulated the electric field to reveal the current distribution in the machining gap for WECMM with a rotary helical electrode and experimentally investigated the effects of the rotary helical electrode and the process parameters on the machining accuracy. When a cylindrical electrode was used, the electrolyte electrical conductivity, was higher in the middle than at both ends of the machining gap but when a rotary helical electrode was used and rotated anticlockwise, the electrolyte axial velocity directed to downward and the electrolyte conductivity was larger at the bottom of the machining zone. Clockwise rotation of the helical electrode was preferred because electrolyte conductivity was almost same in the depth direction. Simulation study showed that a helical electrode could fabricate a narrower slit than a cylindrical electrode with the same diameter as the current density was less and fluctuated in regular interval because of the groove shapes on the helical electrode. The experiments were conducted with a dextral microdrill of diameter 0.3 mm on plates of 3-mm-thick

stainless steel 304. The experimental results revealed that with the increase of the spindle speed, the machining gap first decreased and then increased gradually. As the spindle speed increased, the achievable maximum feed rate increased from 4 to 7 $\mu\text{m/s}$, using a helical electrode and 4 to 8 $\mu\text{m/s}$, using a cylindrical electrode. The results verified with the simulation study and the rotary helical electrode had a smaller interelectrode gap than the cylindrical electrode. Low voltage, low duty cycle, high frequency and low electrolyte concentration were suggested for stable and precision machining. The comb-like microstructure of 3 mm thick with a slit width of 350 μm was fabricated with electrode feed rate of 2 $\mu\text{m/s}$ and the spindle speed of 5000 rpm. A 5 \times 5 array of multiple pins on a substrate with dimensions of 3 \times 3 mm was also fabricated and the micropins were 150 \times 80 μm in size and 2000 μm in height.

Xianghe et al. [15] proposed a method for in situ fabrication of a ribbed wire electrode with large length to diameter ratio (L/D ratio) to avoid the general positioning and machining errors caused by moving and holding the parts by fixture more than once. A 500 μm diameter stainless steel wire electrode on which the ribbed micro structures were to be fabricated was immersed and rotated in the NaNO_3 electrolyte and acted as anode during rib fabrication process. With the feed motion of the tensioned 100 μm diameter molybdenum wire, mounted in a small slot on the wire clamping apparatus, a groove was electrochemically machined on the stainless steel wire electrode and accordingly a series of ribbed structures were fabricated. During wire fabrication process it was found that low pulse duty ratio and electrolyte concentration and high pulse frequency confined the ribbed groove size and accurately fabricated the shape of the rib. The optimal parameters for the wire fabrication process were found to be pulse frequency of 100 kHz, duty cycle of 10% and electrolyte concentration of 15 g/L. The averaged groove width and the averaged depth of the fabricated wire were 113 μm and 100 μm , respectively. Furthermore, the fabricated ribbed wire electrode was utilized in the machining of 20 mm thick stainless steel block to fabricate high-aspect-ratio microstructures. During machining process, the ribbed wire electrode was rotated at high speed and reciprocated in the axial direction and acted as cathode. The machining parameters were an applied voltage of 21 V, a pulse frequency of 100 kHz, a pulse duty cycle of 40%, a NaNO_3 electrolyte concentration of 15 g/L, an electrode feeding rate of 1 $\mu\text{m/s}$, a reciprocating frequency of 1.5 Hz, reciprocating amplitude of 20 mm and a

rotational rate of 5000 rpm. Microstructures with average wall width of 230 μm and the aspect ratio up to 87 were successfully fabricated.

He et al. [16] studied the feasibility of machining γ -TiAl alloy (Ti-42Al-6V-1Cr) using WECM with axial electrolyte flushing. A cathode of 100- μm diameter molybdenum wire and a mixture of NaCl and NaNO₃ electrolytes were used in the process. Variations in the side gap with the electrolyte concentration, applied voltage, pulse period, pulse duty cycle, and feed rate were evaluated. The experimental results showed that as the electrolyte concentration was too low, the material removal rate (MRR) was lower than the feed rate, resulting in the appearance of short circuits and sparks. If the applied voltage was too low, the machining gap was extremely small and a narrow machining gap could lead to difficulty in removing the electrolysis products completely from the machining area. Increasing the pulse duty cycle increased the MRR and enlarged the side gap and if the duty cycle was too low, sparks and short circuits occurred due to the slow MRR. The machining accuracy decreased with increases in the pulse period when the other machining parameters were unchanged. The authors concluded that the charging number of electric double layer within the same time frame decreased with increases in the pulse period, resulting in an increase in the average current and loss in accuracy. The results also revealed that machining accuracy improved as the feed rate increased but if the feed rate was too high, it was difficult for the flushing electrolyte to carry away the electrolysis products from the extremely narrow machining gap effectively, leading to sparks. To ensure the efficiency, accuracy, and stability of the machining process, the optimum combination of parameters was determined to be electrolyte concentration of 1.0 % NaCl and 1.0 % NaNO₃, applied voltage of 17 V, pulse period of 10 μs , pulse duty cycle of 20 %, and feed rate of 3.0 $\mu\text{m/s}$. With the optimum parameter combination the authors fabricated a rectangular channel, the width and depth of which were 3 and 2.5 mm and a triangular channel, the width and depth of which were 4 and 2 mm and a complex-shape slit with an aspect ratio of about 31.

Xiaolong et al. [17] suggested multiple wire electrochemical micromachining (MWECMM) to increase the efficiency in machining arrayed micro structures and analyzed the principle of double layer charging process. Multiple tungsten wires fixed on a clamp was fed into the workpiece of stainless steel 304 of thickness of 100 μm with

a stable federate of $0.1\mu\text{m/s}$ and the electrolyte was 0.05 mol sulfuric acid solution. Experiments were conducted to obtain the waveforms of charging potential between the electrodes applied with different ultrashort voltage and each electrode machining branch in MWECMM was considered to be connected into the circuit in parallel. It was observed from the results that the charging potential increased with the charging time and with the increase of wire electrode amount, the charging rate decreased as well as the maximum charged potential. Because of the pulse generator's characteristics, the steady-state potential decreased with the increase of the wire electrode number and the actual applied voltage on each wire electrode branch decreased as well as the machining current. The authors suggested longer pulse on time and larger pulse amplitude for stable MWECMM process with more wire electrodes. It was found that keeping pulse on time at 80 ns , three wire electrodes could be employed optimally and the machining efficiency could be enhanced to be twice that of using a single wire electrode. Furthermore, an arrayed tree-like microstructure was successfully fabricated in MWECMM with three wire electrodes simultaneously.

Zhu et al. [18] proposed the in situ fabrication of the wire electrode to avoid the problem of wire breakage and to ease the fixation of the wire onto the machining system because very thin wire is used in the WECM process. The mechanism of the machining process was studied and a mathematical model was developed. 2Mol NaOH solution at the temperature of 30°C was used to fabricate a tungsten wire with the initial diameter of $30\mu\text{m}$. Authors in situ fabricated micro wire electrode with the diameter of $5\mu\text{m}$ and it took about 25min to produce this wire electrode. The real-time diameter of tungsten wire was monitored using a relationship between the resistance of the tungsten wire and the diameter. Authors carried out experiments on a nickel plate with the thickness of $80\mu\text{m}$ with the above mentioned fabricated wire in 0.1Mol HCl electrolyte solution and produced micro structures with the slit width of less than $20\mu\text{m}$. The slight vibration of workpiece with the frequency of 5HZ by PZT (piezoelectric ceramics) along the direction of the wire electrode length was employed for effective refreshing of electrolyte in the machining area. Finally authors fabricated a series of complex micro structures with the slit width of $20\mu\text{m}$.

Wang et al. [19] adopted axial electrolyte flow whose direction was assumed to be along the axis of the wire electrode, to renew electrolyte in the machining gap while

fabricating high aspect- ratio slit micro-structures. The wire electrode fixture of axial electrolyte flow was developed accordingly. Tungsten wire electrode of diameter 20 μm was used as the cathode tool to machine work-piece material 0Cr18Ni9 of thickness 5mm in NaNO_3 electrolyte solution. The feed rate of wire electrode and the electrolyte flow rate in the pump output mouth were also modelled. Through theoretical analysis and comparative experiments, it was revealed that processing stability and machining efficiency could be improved by a higher electrolyte flow rate. Optimized process parameters were found to be 1.0 m/s electrolyte flow rate, 10 V applied voltage and 10 g/l NaNO_3 electrolyte. With optimized parameters, structures of micro curved flow channel and micro spline with the aspect ratio of 31 were fabricated on 5-mm-thick stainless steel. The authors also found that lower initial machining gap could decrease the stray current, resulting in a better entrance shape.

Volgin et al. [20] developed the methods of numerical simulation of wire electrochemical machining with regard for possible topological changes in the workpiece surface and studied various schemes of formation of typical features such as slits and openings of various shapes. The model of the wire electrochemical machining involved the Laplace equation for the electric field potential, equation of workpiece surface evolution, and equation of the trajectory of wire tool-electrode. The numerical solution was simplified by using the quasi steady state approximation. The results of modelling showed that the proposed scheme of numerical simulation of wire electrochemical machining was sufficiently effective and could be used to predict the dimensions and shape of workpiece surface and to improve the trajectory of tool-electrode.

1.6 Objective and scope of present research

From literature surveys, it can be understood that the commercial application with WECM is still a challenge with other commercially established Micro fabrication process, where Multi-wires with WECM gives the power to overcome the limitations of WECM in mass production capacity.

Hence, keeping in view of the above, the objectives of the present research work are as below.

- (i) To develop an experimental setup of Multi-wire Electrochemical Machining (MWECEM) which may consists of several subunits such as multi-wire electrodes holding device, machining chamber, electrolyte flow system, power supply, motion control unit, vibration control unit etc. for carrying out experimental investigation.

- (ii) To develop mathematical model for slit width considering double layer charging theory for a particular parameter setting of MWECEM and considering effects of process parameters like wire feed and also validate the mathematical model of slit width with experimental results considering different electrolyte flushing strategies.

- (iii) To investigate experimentally the effects of different electrolyte flushing strategies on slit width and accuracy of machining with varying wire feed rate keeping other process parameters fixed during MWECEM operation.

- (iv) To establish the comparison between different electrolyte flushing strategies with multi wire electrodes in WECEM for selecting best suitable technique for flushing into inter electrode gap during machining.

- (v) To generate complex micro features using MWECEM process considering best parameter setting as obtained from in-depth experimentation.

Multi-wire Electrochemical Machining has potential for applications in the various advanced engineering fields. MWECEM can fabricate complex micro features from wide ranges of materials. In this process wire is not eroded and can be reused and having less diameter and it is environment friendly process. High aspect ratio complex micro structures can also be generated by MWECEM process with high quality and productivity.

2. FUNDAMENTALS OF MULTI-WIRE ELECTROCHEMICAL MACHINING (MWECEM)

2.1 Principle of Multi-wire Electrochemical Machining (MWECEM)

There have been many investigations of WECM, its application in industry is still limited because of its relative low machining efficiency. However, in previous research using the axially vibrating tool, it was only possible to machine a thin work piece a few hundreds of micrometres in thickness at a quite slow feed rate because of limitations on the vibration velocity and amplitude in WECM using ultra-short voltage pulses. In many high-precision devices, array microstructures are commonly used to perform specific functions, such as comb structures in micro-actuators and multiple slits in X-ray phase-contrast imaging systems. The main limitation on the use of WECM to produce these microstructures is that the process is very time-consuming on account of the long machining length. WECM using multi-wire electrodes, named as Multi-wire electrochemical micromachining (MWECEM) in which multiple features of the same shape are fabricated in one process, is a perfect method to improve machining efficiency when fabricating array microstructures at high demand.

Figure 2.1 shows a schematic diagram of MWECEM process. The wire electrodes are arranged in a row and electrically connected to the pulse generator. The principle of MWECEM using axial vibration-assisted multi-wire electrodes which are mounted on tool holder in equal intervals. The work piece acts as the anode and multi-wire electrodes connected in parallel with each other act as the cathodes. In the process, the tool vibrates along its axial direction with high traveling speed, which is the linear speed of moving wires up and down. The electrode motion causes fresh electrolyte to be dragged into the machining area while dirty electrolyte containing electrolysis products (hydrogen bubbles and hydroxides) is dragged out as shown in Fig. 2.1, resulting in the improvement of mass transport rate in the narrow machining gap. The axis of the wires are kept in the same plane by a special fixture. During the machining process, all the

wires follow the same path at a constant feed rate and cut the work piece simultaneously.

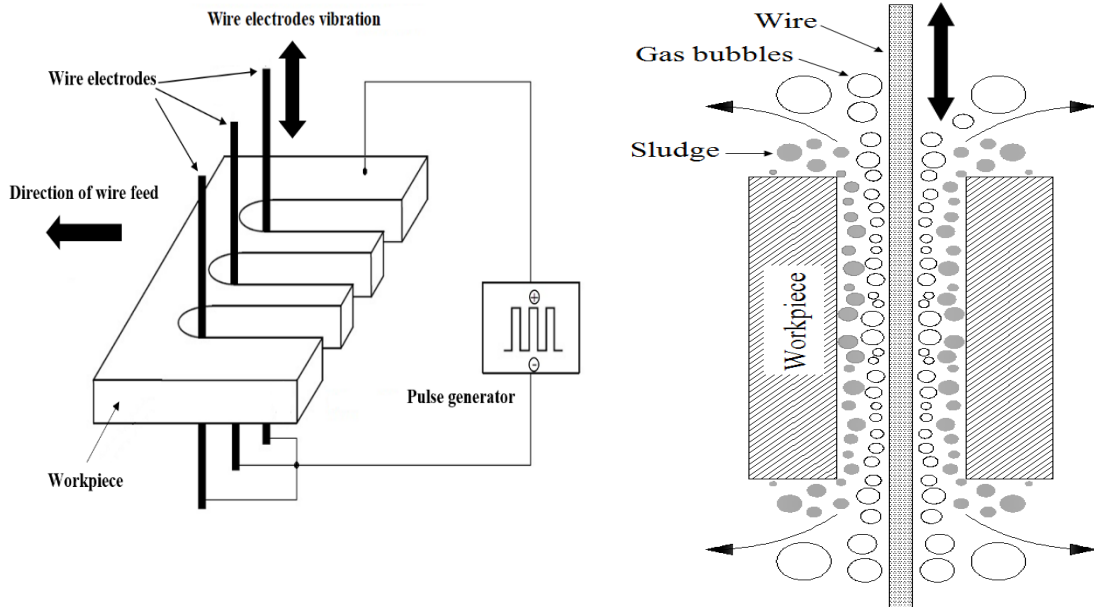


Fig. 2.1 Schematic diagram of axial vibration-assisted Multi-wire Electrochemical Machining

In the machining process, the wire electrodes are feeding along the programmed tool path simultaneously. Once short-circuits occur between the workpiece and one of the wire electrodes, the whole machining process should be halted. Therefore, it is important to ensure that the machining status of each electrode branch is same with each other in MWECEM process.

As shown in Fig. 2.1, multiple wire electrodes electrochemical micro machining is a method for fabricating several metal micro slits or structures simultaneously. It uses arranged wire electrodes. During the machining process, an appropriate voltage is applied between the workpiece and the wire electrodes. At the anodic workpiece surface, metal is dissolved into metallic ions by electrochemical reactions. As one of the wire electrodes is short-circuited, the machining process should be expelled, and all the wire electrodes must respond quickly, the machining gap of each wire electrode

machining branch must be controlled over a reasonable range to facilitate the stability of the multiple wire electrode electrochemical micro machining process.

2.2 Different machining conditions in Multi-wire Electrochemical Machining (MWECEM)

(i) Effects of number of wire electrodes

The slit width decreases and the total average machining current increases with increasing number of wire electrodes. When the same pulse on-time is applied, the feed rate decreases with increasing number of wire electrodes. When the number of tool electrodes increases, the cell impedance decreases because the polarization resistance decreases and the double layer capacitance increases. Therefore, when the feed rates are the same, a greater number of tool electrodes requires longer pulse on-times for successful machining.

(ii) Effects of Applied Voltage on Machining

The average slit width increases with the increase of applied voltage and the uniformity of slit width also decrease with applied voltage.

(iii) Effects of Pulse On-time on Machining

The standard deviation of the slit widths increases with pulse on-time. Put another way, the uniformity of the slit widths decreases with increasing pulse on-time. The average slit width increases with the pulse on-time. Although the increase of pulse on-time can increase the faradaic current and the metal electrochemical dissolution volume, the removal of the products near the anode in the machining gap becomes difficult. Electrolytic product accumulation increases the probability of large fluctuations of electrolyte conductivity, leading to a reduction in the uniformity of the slit widths.

(iv) Effects of Pulse Period on Machining

When the pulse on-time is a constant, for each pulse, almost the same amount of bubbles are generated. In a short pulse period, the pulse off-time is short. Therefore, the overflow time of small bubbles is shorter, and small bubbles

easily accumulate between the wire and the workpiece. When the size of the accumulated bubbles increases, the wire can be deformed due to the surface tension of the bubbles. Moreover, the bubbles prevent ion diffusion or flushing of the electrolyte, which produces irregular shapes.

(v) Effects of Feed Rate on Machining

With increasing feed rate slit width is reduced, but too high feed rate deteriorates the stability of machining. At low feed rate, the accuracy of slit width is very poor.

2.3 Equivalent Circuit for Multi-wire Electrochemical Machining (MWECEM)

Actually, the MWECEM system is an electrical circuit. The anodic workpiece, the electrolyte and the cathode wire electrode comprise as a system to be part of the circuit. Figure 2.2 presents a schematic diagram and equivalent circuit of distributed capacitances and resistances between the electrodes in MWECEM process. In details, there are double layer capacitance, C_d , remains in parallel with faradaic reaction impedance that consists of active charge transfer resistance, R_{ct} and Warburg resistance, R_w . The total double layer circuit consists of two of these types of circuits, one for cathode and another for anode. These two circuits remain in series with active electrolyte resistance i.e. the resistance of electrolyte between anode and cathode, and represent the total double layer equivalent circuit for single wire system formed in the machining gap. This equivalent circuit is converted into equivalent circuit for Multi-wires electrodes. When the ultrashort voltage pulse is the same, the difference between WECM using a wire electrode and MWECEM is the time constant and the electrode amount.

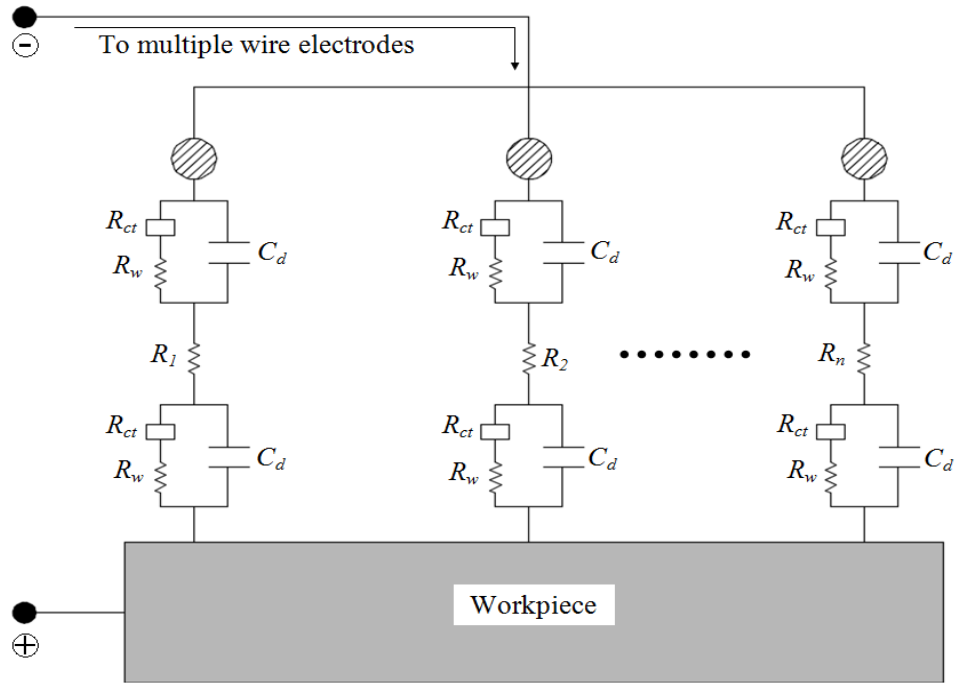


Fig. 2.2 Equivalent Circuit for Multi-wire Electrochemical Machining

In the equivalent circuit of MWECEM as shown in Fig. 2.2, the distribution of capacitance and the resistance is quite complex. If the time constant is longer than the pulse on time t_{on} , the potential possibly could not be charged up to the material removal potential level. And the situation will change with the wire electrode amount.

According to Ohm's law and the equivalent circuit for MWECEM as shown in Fig. 2.2, the machining voltage increases with decreasing number of electrodes, leading to the increase in machining current (I). Assuming that the widths of the machined multiple slits are almost equal to each other, and thus the average current for each electrode, I_{each} , is the same and can be calculated as

$$I_{each} = I / n$$

The average current for each electrode decreases with increasing number of electrodes (n), which is consistent with the above analysis. As a consequence, the MRR is larger when there are fewer electrodes, resulting in a wider slit. A wider slit favours mass transport in the machining gap. Owing to the higher MRR and the greater mass transport efficiency, a higher feed rate can be applied when there are fewer electrodes.

2.4 Advantages of Multi-wire Electrochemical Machining (MWECM)

Although there have been many investigations of WECM, its application in industry is still limited because of its relative low machining efficiency. A method namely Multi-wires electrochemical micromachining (MWECM) had been proposed to increase the productivity in machining arrayed structures. MWECM employs an array of metallic wires as the cathode, thus an array of microstructures could be machined simultaneously. WECM using multi-wire electrodes, in which multiple features of the same shape are fabricated in one process, is a perfect method to improve machining efficiency. In this way multi-wire electrochemical micromachining will play an important role to improve the machining productivity of WECM. The other advantages of MWECM is same as the WECM process are listed below:

- (i) High aspect ratio complex microstructures can be easily fabricated by WECM process.
- (ii) Unlike other EMM processes, complex tool fabrication process is not needed in WECM.
- (iii) Tool for WECM is a wire with diameter generally less than 100 μ m. The wire materials that are available for WECM are tungsten, copper, platinum and molybdenum. Cost of the wire is relatively less in comparison of with tools used in other EMM process.
- (iv) Micro features formed by WECM process do not have tapering effect.
- (v) As the wire with diameter in micron ranges are used, very small and precise dimensions can be achieved.
- (vi) Production rate is higher as less time consuming and associated cost is lower in WECM process, and
- (vii) Better surface integrity can be achieved by WECM, etc.

2.5 Applications of Multi-wire Electrochemical Machining (MWECM)

Multi-wire Electrochemical Machining has very high potential for application in the aeronautics, automobile, electronic and biomedical industries. High aspect ratio complex shaped micro structures and high productivity which are needed for MEMS applications, have been fabricated by MWECM process. MWECM can fabricate micro features from wide ranges of work piece material. Different complex shaped micro

features such as micro-fins, micro-cam, micro-gear, micro-helix etc. have been fabricated. It can be superior to Wire-EDM process in mass production.

Still MWECM is not yet fully developed process to be used in the industrial applications. Extensive research work in different aspects of MWECM is still needed so that MWECM can be used as a fully functional process in different industries.

3. DEVELOPMENT OF MULTI-WIRE ELECTROCHEMICAL MACHINING (MWECEM) EXPERIMENTAL SETUP

To develop the MWECEM set-up, various components with different sub-systems are assembled together as well as developed according to the requirement so that the experimentations can be performed on the developed MWECEM set-up. The developed setup is shown in Fig. 3.1, where different subsystems are exhibited.

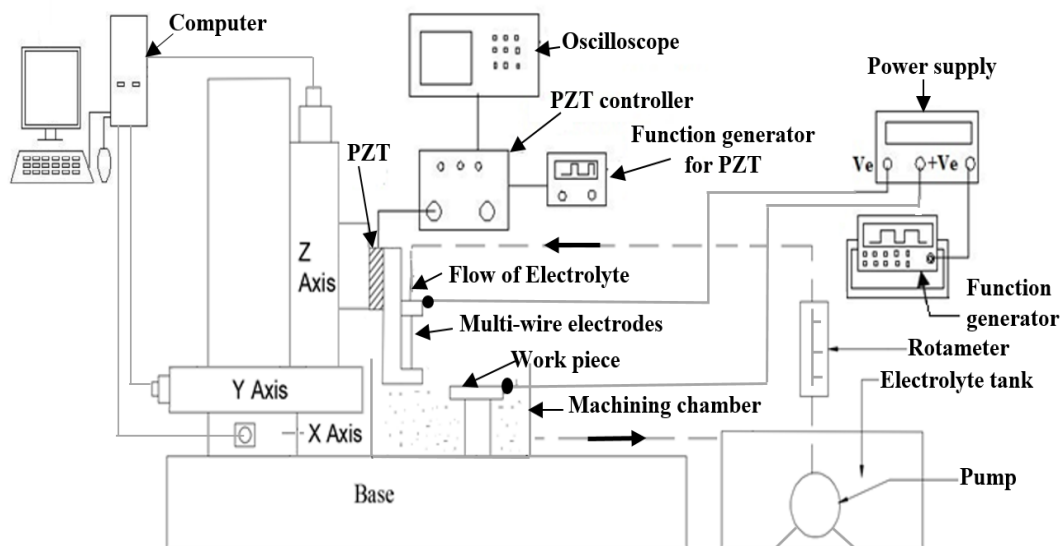


Fig. 3.1 Schematic diagram of the developed MWECEM set up

3.1 Various developed components of Multi-wire Electrochemical Micromachining (MWECEM)

To develop the setup of MWECEM process, various components have been developed and assembled for performing in-depth experimentation into MWECEM process. The details of sub components are as follows:

3.1.1 Multi-wires holding device

A special type of multi wires holding device has been developed to clamp the tungsten wire. Wire is held vertically and firmly in the mentioned block. Maximum 10 tungsten wires with 500 μ m spacing is the capability of this wire holding device. This wire

holding device is mounted via an attachment on the Z-axis of the movement stage mentioned above. It is also made of Acrylic sheet for easy monitoring and control. Moreover, the wire holding device has arrangement to attach it with Piezo Electric Transducer (PZT). In addition, suitable axial electrolyte flow system has been developed and incorporated on the wire holding device for supplying axial flow. This flow system also has arrangements for regulating and positioning of the flow as shown in Fig. 3.1.

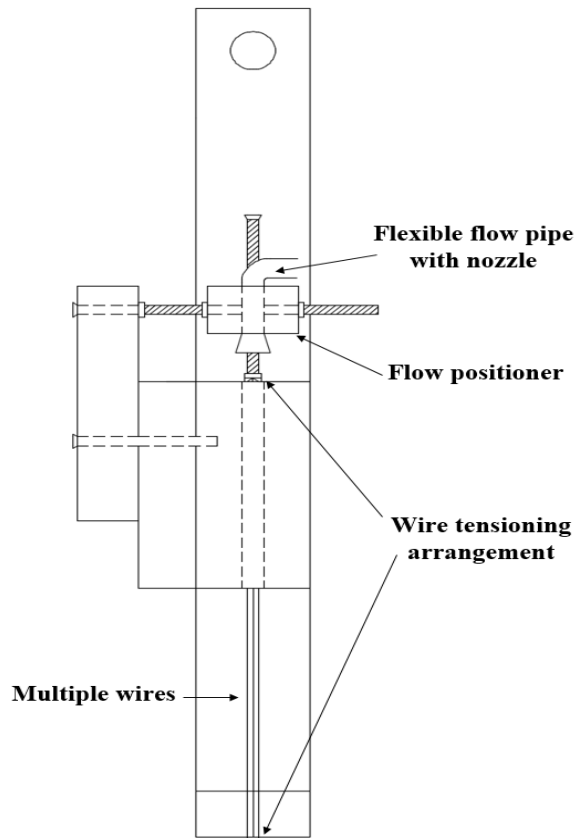


Fig. 3.1 Schematic diagram of the developed Multi-wire holding block

3.1.2 Machining chamber

The schematic diagram of the developed machining chamber is shown in Fig. 3.3. The machining chamber is placed on the worktable during experiments to hold the required electrolyte solution and work piece. There is a breadboard of M6 thread on the worktable to hold the machining chamber and to restrict its movement during experimentations. The machining chamber is attached by means of M6 screws and nuts. The machining chamber is made of non-conductive and non-corrosive acrylic sheet which will not react with the acidic electrolyte. Acrylic has been selected because of its

transparency which will help in easy monitoring and controlling of the process. For easy removal of electrolyte after machining and during machining, an outlet at base level of the chamber has been also provided on one side. Furthermore, there is a special arrangement for work piece clamping and holding in the machining chamber. This special arrangement has been made in such a way that it would prevent the undesired vibration generated due to the flow of the electrolyte.

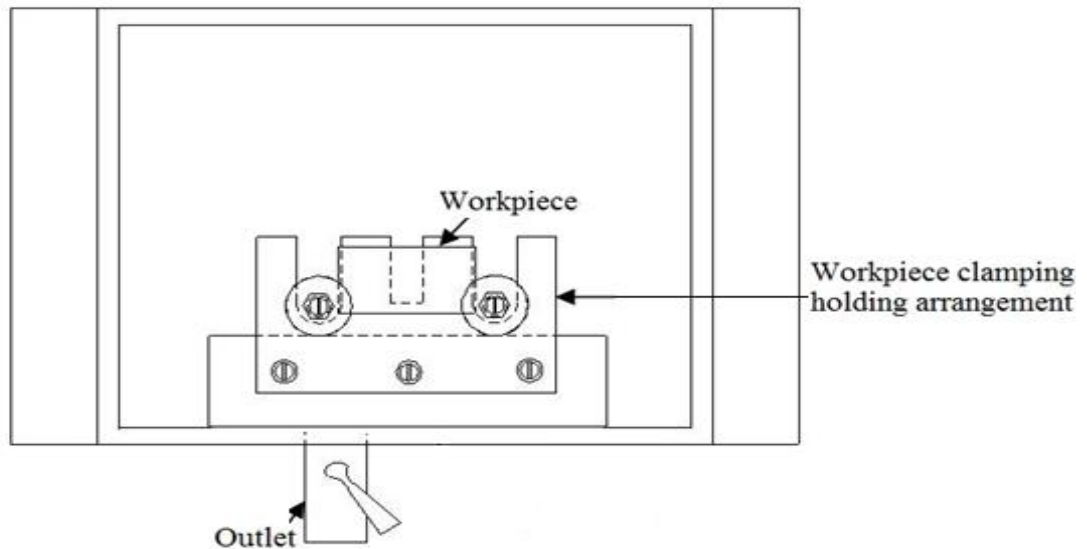


Fig. 3.3 Schematic diagram of the developed machining chamber

3.2 Various sub-systems of Multi-wire Electrochemical Micromachining (MWECEM) set-up

Experimental setup for WECM consists of various sub-systems such as XYZ movement stage, power supply unit, vibration unit etc. Various components of these sub-systems which have been attached with the developed components to complete the experimental set-up, are discussed here in brief.

3.2.1 XYZ movement stage

MTN100PP XYZ Movement stage made by Newport Corporation, having travel range 100 mm and minimum incremental motion is 0.1 μm . A mounting attachment is present with the Z-axis to carry the wire holding block. Three different stepper motors provide the drive for the XYZ stage. Axial load carrying capacity of Z axis along gravity is 200 N and opposite of gravity is 21 N.

3.2.2 Power supply unit

The power supply unit consists of function waveform generator and amplifier. Details of those components are discussed in brief here.

(i) Function waveform generator

33250A function waveform generator made by Agilent has been used for experimental work. This waveform generator uses direct digital-synthesis techniques to create a stable, accurate output on all waveforms, down to 1 μ Hz frequency resolution. This waveform generator generates the desired waveform such as sine square, pulse, ramp etc. with desired pulse parameter setting which is feed to the bi-polar amplifier. For MWECEM experimental work, the desired waveform that has been selected is pulse waveform. Pulse frequency in the range of 500 μ Hz to 80 MHz and pulse period in the range of 20ns to 2000s are offered by this function waveform generator. Moreover, function waveform generator provides pulse width in the range of 8ns to 1999.9s.

(ii) Amplifier

POA 75-4 rackmount bi-polar power supply made by Matsusada Precision Inc., is used as the amplifier. The pulse waveform generated from the waveform generator discussed above is fed to the amplifier and the resultant output from the amplifier has been used during machining. This amplifier provides voltage in the range 0 to ± 75 V maximum current 4A and maximum pulse frequency 1MHz.

3.2.3 Vibration unit

nanoSX400 high speed piezo X-positioner made by Piezosystem jena GmbH, Germany was used as the vibration unit. This provides motion range upto 400 μ m. This vibration unit was attached with the Z stage for experimentation. Nano SX400 piezo has 0.8 nm motion resolution and maximum load carrying capacity is 10 Kg.

3.2.4 Ancillary unit

Different accessories like multimeter, oscilloscope have also been used to serve different purpose during experimentations of WECM. These accessories are discussed here in brief.

For measuring the machining current during experiments, multimeter is used. It is made of Tektronix, USA. It can also be used for measuring the value of capacitance.

To monitor the pulse pattern and to analyse the nature of pulse, oscilloscope with facility to store digitally the pulse power parameters, is used during experiments. The oscilloscope is Tektronix TBS 1062 and has a bandwidth of 60 MHz with a sampling rate of 1 GS/s.

To measure the flow rate through the pipe rotameter is used and its reading showing in the lph scale in the range of 15 to 60 lph.

Development of multi-wire electrode holder and axial electrolyte flushing attachment is completed successfully, where various subsystems like PZT, power system, function generator, oscilloscope, rotameter, submersible pump are here with assembled to complete the MWECM setup that can forward MWECM process for successful experimentation in a fruitful way.

The overall photographic view of the developed MWECM set-up is shown in Fig. 3.4. The photographic view of the developed Multi-wire holding block is shown in Fig. 3.5.

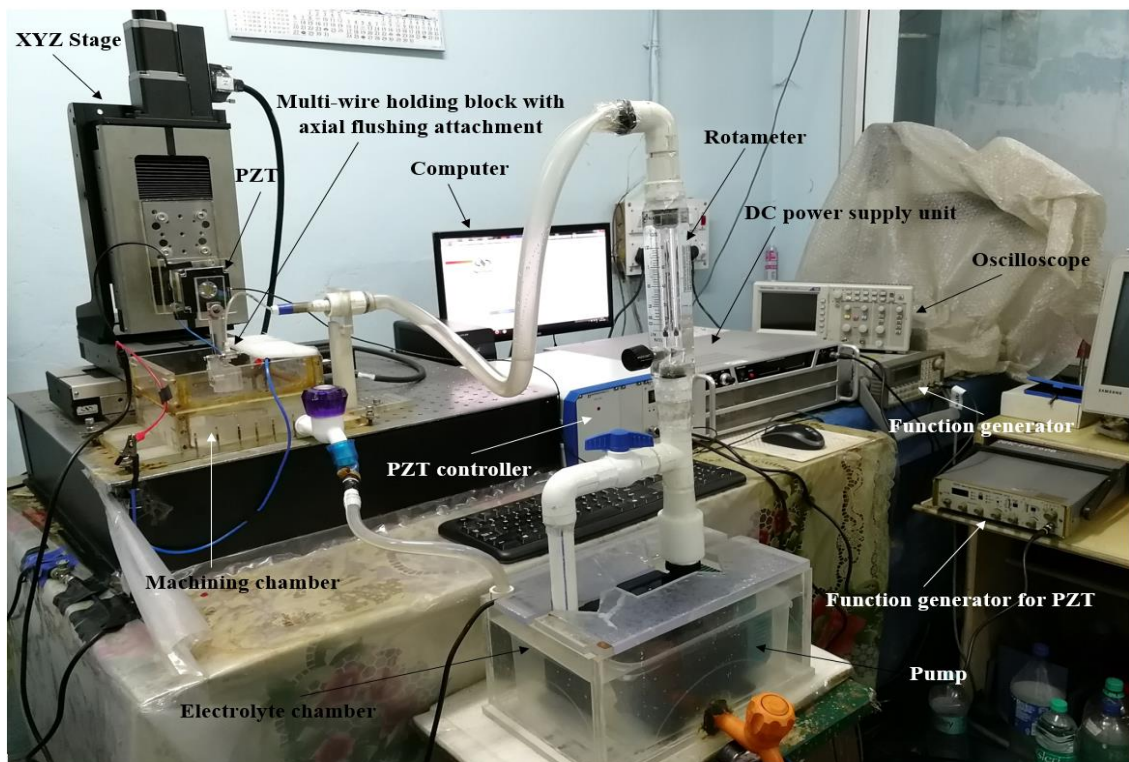


Fig. 3.4 Photographic view of the developed MWECM set-up

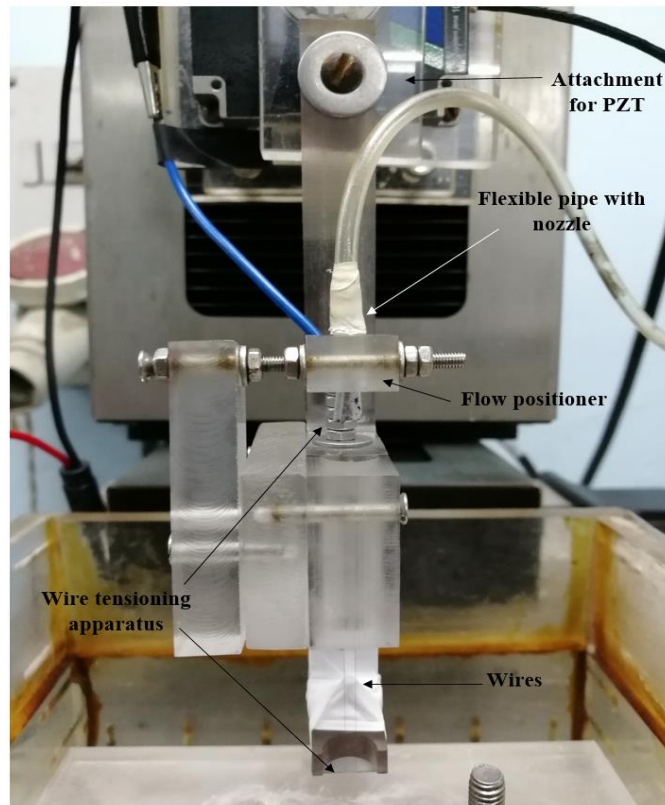


Fig. 3.5 Photographic view of the developed Multi-wire holding block

4. DEVELOPMENT OF MATHEMATICAL MODELLING FOR MULTI-WIRE ELECTROCHEMICAL MACHINING

Mathematical model has been developed to theoretically analyse different aspects of MWECM. In this model the correlation among duty ratio, applied frequency, applied voltage, feed rate and generated slit width has been obtained with different number of wire electrodes.

4.1 Correlation of the process parameters with the width of the micro slit

The feature dimensions and geometry of the fabricated micro feature greatly depends upon the operating parameters involved in MWECM for which proper control of involving parameters is necessary to attain desired output. Hence, in this research work a mathematical model has been developed to obtain a theoretical relationship between the width of the generated micro slit and process parameters like frequency, duty ratio, applied voltage, feed rate with different number of wire electrodes.

The changing position of tool wire with increase in machining duration and equivalent circuit model for generated double layer is shown in Fig. 4.1. The cathode wire is fed forward in its radial direction into the anode work piece making a slit width of W_s . The double layer circuit is based on Randles circuit, where double layer capacitance, C_d , remains in parallel with faradaic reaction impedance that consists of active charge transfer resistance, R_{ct} and Warburg resistance, R_w . The total double layer circuit consists of two of these types of circuits, one for cathode and another for anode. These two circuits remain in series with active electrolyte resistance i.e. the resistance of electrolyte between anode and cathode, and represent the total double layer equivalent circuit for single wire system formed in the machining gap. This equivalent circuit is converted into equivalent circuit for Multi-wires electrodes. However, the side inter electrode gap δ_{sg} is larger than frontal inter electrode gap δ_{fg} . So, R_I' which is the active electrolyte resistance for side gap is different from R_I which is the active electrolyte resistance for front gap. But, as the differences are very negligible, so, for ease of calculation it can be assumed that $R_I \approx R_I'$.

Same as WECM, MWECM is an anodic dissolution process, so, the material removal is governed by Faraday's law which gives,

$$m = \frac{Alt}{zF} \quad (1)$$

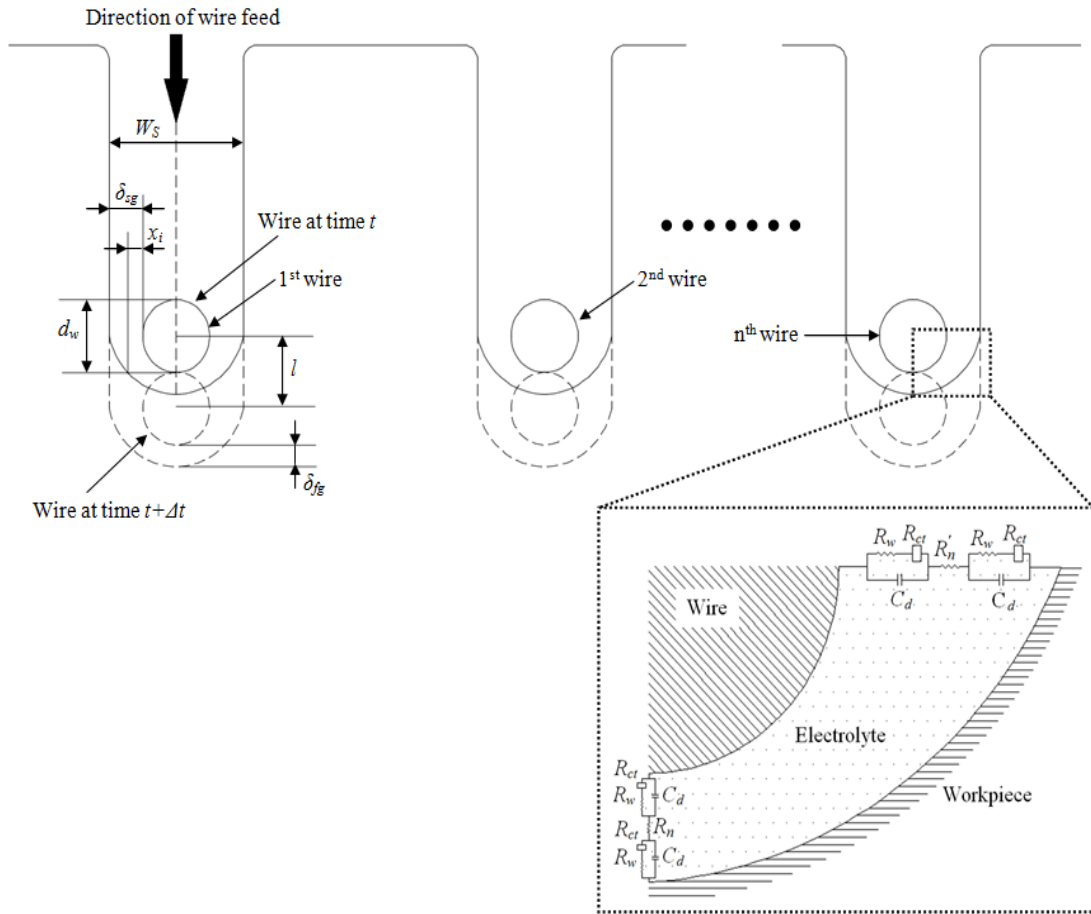


Fig. 4.1 Position of multi-wires with the increase in machining duration and equivalent circuit for the double layer

Where, m is the mass of removed material from anode, A is atomic weight, I is current during machining, t is the machining time, z is the valence of ions of the anode material and F is Faraday's constant.

The Eq. (1) can be re-written as

$$m = \frac{e_a Vt}{R_{eq}} \quad (2)$$

Where, $e_a = A/(zF)$ and is electrochemical equivalent, V is applied voltage, R_{eq} is resistance of the equivalent circuit.

However, the voltage considered in Eq. (2) is constant dc voltage and can also be denoted as V_{dc} . But, as MWECCM operates on pulsed dc voltage so the term duty ratio (D_r) which is the ratio of pulse on time to total cycle time, is very significant and should be included here to obtain the effective voltage responsible for machining. Also, double layer charging time (τ) plays an important role and has been considered in the modelling which is,

$$\tau = \rho C_d \delta_{fg} \quad (3)$$

Where, ρ is resistivity, C_d is double layer capacitance and δ_{fg} is frontal inter-electrode gap.

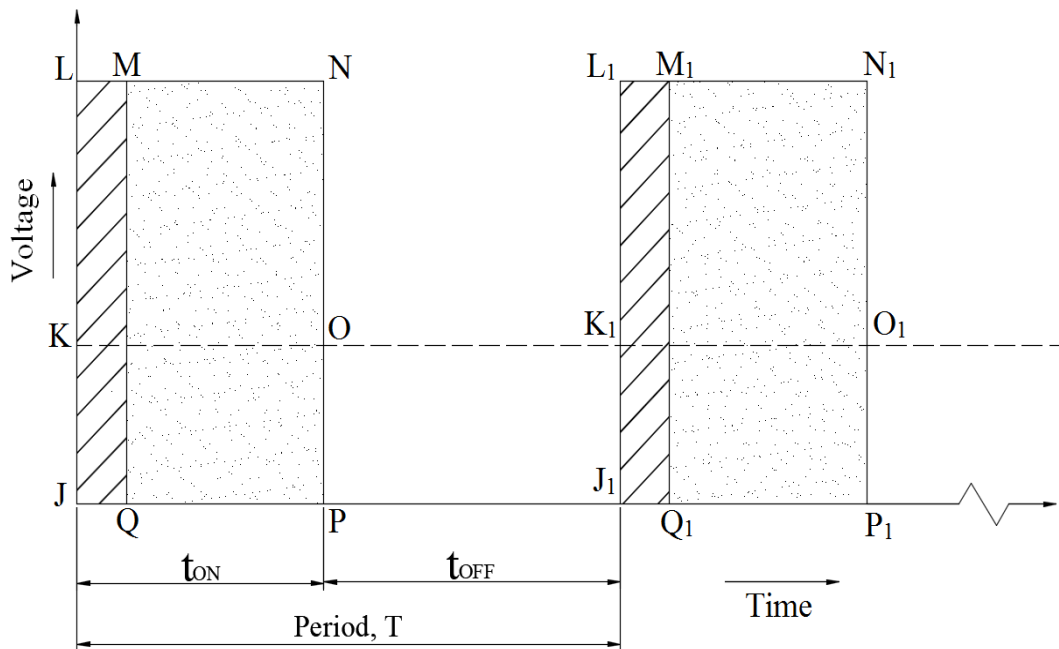


Fig. 4.2 Schematic diagram of voltage pulses during machining

Now, for better understanding, condition of voltage during a particular cycle is shown in Fig. 4.2. JJ_1 is the cycle time period which is denoted by T . But this entire time period is not available for machining. Here, machining only occurs during JP and is denoted as t_{on} . However, during JP , double layer charges and discharges instantly. In Fig. 4.2, JQ is the double layer charging time. Therefore, machining only occurs during QP . From Fig. 4.2, JL is the input pulse voltage and can be denoted as V whereas, only area $QMNP$ is responsible for machining. JK is the equivalent dc voltage, V_{dc} for time period,

T. Here, JK can be chosen in such a way that area of QMNP equals to area of JKK₁J₁.
So,

$$(JK)(JJ_1) = (JL)(QP)$$

Therefore,

$$V_{dc}T = V(t_{on} - \tau) = (D_r - \tau f)V, \text{ where, } D_r = t_{on}/T, f = 1/T \text{ and } f \text{ is applied frequency.}$$

Hence, Eq. (2) can be re-written as

$$m = \frac{e_a(D_r - \tau f)Vt}{R_{eq}} \quad (4)$$

Now, the volume of material removed from workpiece (V_l) is

$$V_l = \frac{e_a(D_r - \tau f)Vt}{R_{eq}\rho_a} \quad (5)$$

Where, ρ_a is the density of the anode material.

Hence, the Eq. (5) can be written as

$$x = \frac{\alpha(D_r - \tau f)Vt}{R_{eq}A} \quad (6)$$

Where, x is the variable of length, $\alpha = \text{volumetric electrochemical equivalent} = e_a/\rho_a$ and A is area of machining.

Differentiating Eq. (6),

$$\frac{dx}{dt} = \frac{\alpha(D_r - \tau f)V}{R_{eq}A} \quad (7)$$

From equivalent circuit model shown in Fig. 4.1 it can be written as

$$\frac{dx}{dt} = \frac{\alpha(D_r - \tau f)V}{\left(\frac{R_1 + 2R_e}{n}\right)A} \quad (8)$$

Where,

$$R_e = \frac{R_{C_d}(R_W + R_{ct})}{R_{C_d} + R_W + R_{ct}} \quad (9)$$

Where, R_{Cd} is capacitive reactance and

$$R_W = \frac{RT}{n^2 F^2 A \sqrt{f}} \left(\frac{1}{C^*_O \sqrt{D_O}} + \frac{1}{C^*_R \sqrt{D_R}} \right) \quad (10)$$

Where, R is the Universal Gas Constant, T is temperature, n_e is the number of electrons transferred, C^* is the bulk concentration of diffusing species and D_O is the diffusion coefficient of the oxidant and D_R is the diffusion coefficient of the reductant, and

$$R_{C_d} = \frac{x_2}{f A \epsilon \epsilon_0} \quad (11)$$

Where, x_2 is the Stern layer thickness, ϵ is the relative permittivity of the solution, ϵ_0 is the permittivity of vacuum and

$$R_{ct} = \frac{RT'}{n_e F i_0} \quad (12)$$

Where, i_0 is the exchange current density

From Eq. (10) and (11) it can be easily found that for high frequency, values of R_W and R_{C_d} are very small. Hence, these values can easily be neglected. Therefore, from Eq. (9), R_e is also negligible.

$$\text{Hence, } R_{eq} \approx R_l \quad (13)$$

Now,

$$R_l = \rho \frac{x}{A} \quad (14)$$

Where, ρ is the specific resistivity and $\rho = 1/K_e$, and K_e is the conductivity of the electrolyte.

$$\text{Here, } R_l = R_2 = \dots \dots = R_n$$

So, from Eqs. (8), (13) and (14) it can be written as,

$$\frac{dx}{dt} = \frac{n \alpha K_e (D_r - \tau f) V}{x} \quad (15)$$

Therefore,

$$x dx = n \alpha K_e (D_r - \tau f) V dt \quad (16)$$

Integrating Eq. (16),

$$\frac{x^2}{2} = n\alpha K_e(D_r - \tau f)V\Delta t + \frac{x_i^2}{2} \quad (17)$$

Now, from Eq. (15), it can be written as,

$$f_w = \frac{n\alpha K_e(D_r - \tau f)V}{\delta_{fg}} \quad (18)$$

Where, f_w is feed of cathode wire.

If, the wire moves l unit in forward direction in time Δt , then

$$\Delta t = l/f_w \quad (19)$$

Now, it is clearly evident from Fig. 4.1 that,

$$l = d_w \quad (20)$$

Where, d_w is the diameter of the wire.

From Fig. 4.1 it is clear that x_i is the side inter electrode gap at time t and is considered as the integration constant. Now, as the diameter of the wire is very small this x_i as well as δ_{fg} i.e., frontal inter electrode gap will also be very small. Hence, it can be assumed as,

$$x_i \approx \delta_{fg} \quad (21)$$

For same reason side inter electrode gap (δ_{sg}) can also be assumed as,

$$\delta_{sg} \approx x \quad (22)$$

Now, from Eq. (18) & Eq. (20) to (22), it can be written as,

$$\frac{\delta_{sg}^2}{2} = n\alpha K_e(D_r - \tau f)V \frac{d_w}{f_w} + \frac{\delta_{fg}^2}{2} \quad (23)$$

Now, from Eq. (18) and Eq. (23), it can be written as,

$$\delta_{sg} = \sqrt{2n\alpha K_e(D_r - \tau f)V \frac{d_w}{f_w} + \left(\frac{n\alpha K_e(D_r - \tau f)V}{f_w}\right)^2} \quad (24)$$

Hence, from Fig. 2, the slit width, W_s can be calculated as,

$$W_s = d_w + 2\sqrt{2d_w \frac{n\alpha K_e(D_r - \tau f)V}{f_w} + \left(\frac{n\alpha K_e(D_r - \tau f)V}{f_w}\right)^2} \quad (25)$$

The above equation provides the relationship between width of the fabricated micro slit, frequency and duty ratio, applied voltage, feed rate with number of wires. Also, the developed model has been theoretically analysed and validated with practical experimental results to prove the correctness of the model as well as effectiveness of the same for industrial applications.

5. EXPERIMENTATION ON MULTI-WIRE ELECTROCHEMICAL MACHINING (MWECEM)

With the developed Multi-wire Electrochemical micromachining setup that is discussed earlier, all the planned experiments are carried out. Results of experiments of MWECEM process are discussed here with different flushing strategies. Moreover, a basic comparison is established among all used flushing criteria in MWECEM process. Thereafter, the developed mathematical modelling of slit width has been validated with experimental results to prove the effect of wire feed rate with different flushing conditions.

5.1 Preliminary Experimentation in Multi-wire Electrochemical Micromachining (MWECEM)

5.1.1 Planning for Preliminary experimentation

At first, with some previous experiments of WECEM it has been optimized that below 9 V applied voltage with 12 % duty ratio machining is not effective for micro slit fabrication., In multi-wire setup, the number of wire electrode is three. Therefore, with 9V voltage at 12 % duty ratio machining may not be fruitful. So, here voltage and duty ratio are considered as 12 V and 12% to continue the MWECEM process with three wire electrodes. After that, sets of preliminary experiments have been carried out taking tungsten wire of diameter 50 μm as cathode in three wire MWECEM setup and stainless steel (SS 304) sheet of thickness 100 μm as anode considering axial flushing technique. All the experiments have been conducted with 0.1 M H_2SO_4 due to the fact that acid electrolyte produces less machining product than normal salt electrolyte.

5.1.2 Results and discussions

To carry out required trial experiments, to define suitable machining conditions and to highlight prime operating parameters for generation of desired micro features, proper scheme has been designed with the utilization of developed MWECEM setup that is

discussed earlier. Here, sets of preliminary experiments have been carried out taking tungsten wire of diameter $50\ \mu\text{m}$ as cathode in three wire MWECM setup and stainless steel (SS 304) sheet of thickness $100\ \mu\text{m}$ as anode. All the experiments have been conducted with electrolyte $0.1\ \text{M}\ \text{H}_2\text{SO}_4$.

Initially, using three wire MWECM system the trial experiment is done at $12\ \text{V}$ voltage, 12% duty ratio, $50\ \text{KHz}$ frequency, $0.9\ \mu\text{m/s}$ feed, $0.1(\text{M})\ \text{H}_2\text{SO}_4$ concentration and $35\ \text{lph}$ axial flushing flowrate.

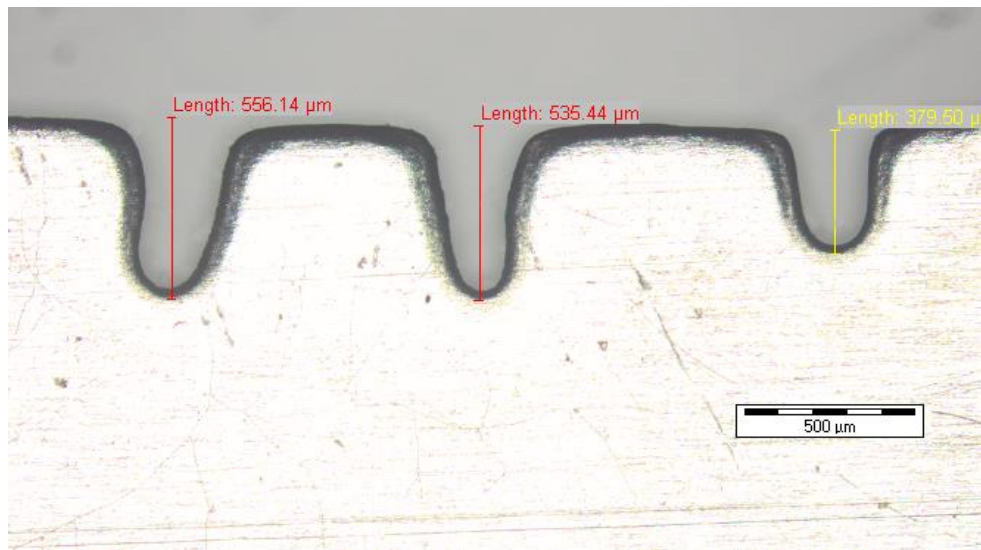


Fig. 5.1 Micro slits machining with three wire W electrodes having $\phi\ 50\ \mu\text{m}$, $12\ \text{V}$ voltage, 12% duty ratio, $50\ \text{KHz}$ frequency, $0.9\ \mu\text{m/s}$ feed, $0.1(\text{M})\ \text{H}_2\text{SO}_4$ concentration and $35\ \text{lph}$ axial flushing flowrate

Here, it is found that due to lack of proper tension in each wire of three during machining, wires are not stable in their positions. As a result, micro slits are not straight and are not same in length as shown in Fig. 5.1. The second effect implies that the alignment of three wires is not in a single plane. This results may conclude that before starting machining with multi-wire setup, alignment of wires must be checked whether they are in same plane or not. Further, this problem is resolved with the help of optical microscope where the three wires are together shown as a single straight line from side view of multi-wire tool holder. Thereafter, taking same parameters of the previous experiment, the modified three wire multi-wire system provides the successful machining as shown in Fig. 5.2.

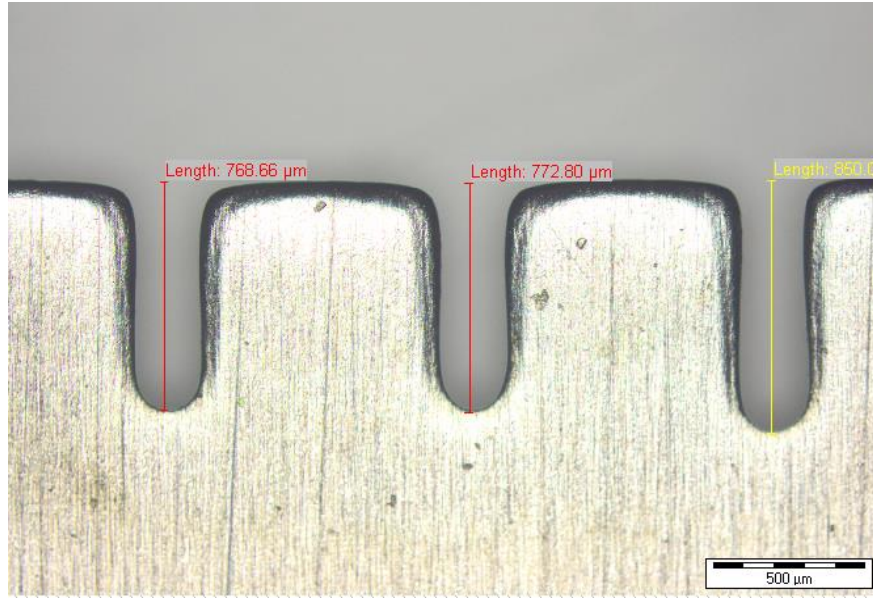


Fig. 5.2 Micro slits machining with three wire W electrodes having ϕ 50 μm , 12 V voltage, 12% duty ratio, 50 KHz frequency, 0.9 $\mu\text{m/s}$ feed, 0.1(M) H_2SO_4 concentration and 35 lph axial flushing flowrate with perfectly aligned of wires

5.2 Axial flushing assisted Multi-wire Electrochemical Micromachining (MWECEM)

With the developed electrolyte flow system, axial flushing of electrolyte is introduced in Multi-wire Electrochemical Micromachining to achieve proper machining without any distortion as it helps in continue supply of fresh electrolyte in the machining zone.

5.2.1 Planning for experimentation

At first, taking the same parameter of successful preliminary experiment where the electrolyte flow rate is taken constant at 35 lph, controlling with rotameter, axial flushing is observed at different feed rate from 0.5 $\mu\text{m/s}$ to 1.5 $\mu\text{m/s}$ and for all the experiments IEG is taken as 100 μm . After completing all this machining with three wire electrodes which are mounted in wire holding block with 1mm spacing in multi-wire electrochemical system at 35 lph electrolyte flow rate, the average slit width is calculated from measured value of slit width of generated micro slits with optical microscope at different feed rate. Then, with the feed rate at which minimum width of micro slit is achieved, has been taken for further observing the effect of other flow rate and which has better performance in axial flushing criteria. This is optimized at 37.5

lph flow rate for rest of the machining. The process parameters for the final experiments are shown in Table 5.1.

Accuracy of slit is represented by the standard deviation of various width of the slit measured along the length of a single slit at different locations. It exhibits the homogeneity of the slit width along the full length of the slit. Standard deviation deviation of slit width is obtained utilising following equation.

$$SD = \sqrt{\frac{\sum_{i=1}^n (x_i - x_{mean})^2}{n-1}}$$

Where, n = number of data,

x_i = each of the value of data,

x_{mean} = mean of x_i

Table 5.1 Process parameters for carrying out final experiments with Axial flushing

Process parameters	Values
Tungsten wire diameter, (μm)	50
Number of wire electrode	3
Stainless steel sheet thickness, (μm)	100
Initial inter electrode gap, (μm)	100
Voltage, (V)	12
Electrolyte	H ₂ SO ₄
Electrolyte concentration, (M)	0.1
Frequency, (KHz)	50
Duty ratio, (%)	12
Wire feed rate, ($\mu\text{m}/\text{sec}$)	0.5 – 2.1
Electrolyte Flow rate, (lph)	37.5

5.2.2 Results and discussions

Initially, the electrolyte flow rate is taken constant at 35 lph, controlling with rotameter, axial flushing is observed at different feed rate from 0.5 $\mu\text{m}/\text{s}$ to 1.5 $\mu\text{m}/\text{s}$ and for all the experiments IEG is taken as 100 μm . After completing all this machining with three wire electrodes which are mounted in wire holding block with 1mm spacing in multi-wire electrochemical system at 35 LPH electrolyte flow rate, the average slit width is calculated from measured value of slit width of generated micro slits with optical microscope at different feed rate and are plotted them on graph as shown in Fig. 5.3. Here, it is clear that at feed rate 1.3 $\mu\text{m}/\text{s}$ the average slit width is minimum. In fig. 5.4

it is found that at 1.5 $\mu\text{m/s}$ feed the machining is worse and not in full length with the presence of short circuit. It also represents the limitation of feed rate in machining at 35 lph flow rate.

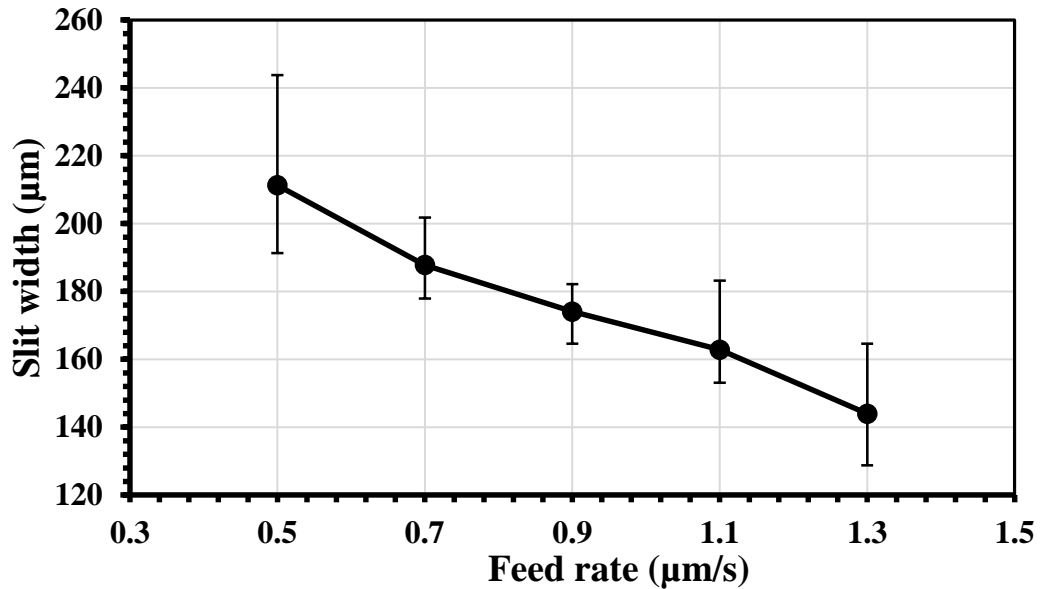


Fig. 5.3 Effect of wire feed on slit width with 35 lph Axial flushing

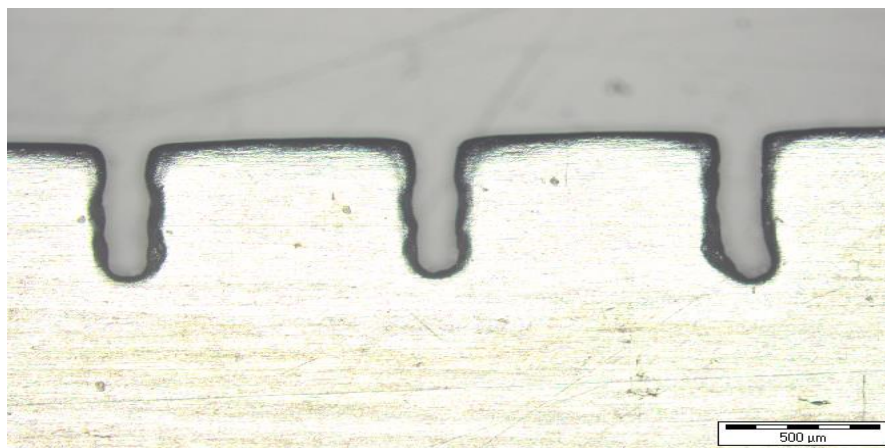


Fig. 5.4 Micro slits machining with three wire W electrodes having ϕ 50 μm , 12 V voltage, 12% duty ratio, 50 KHz frequency, 1.5 $\mu\text{m/s}$ feed, 0.1(M) H_2SO_4 concentration and 35 lph axial flushing flowrate

It is clear from Fig. 5.4 that at high wire feed, three wires system is unable to continue good machining in full length due to insufficiency of electrolyte in machining zone of inter electrodes at 1.5 $\mu\text{m/s}$ feed rate with 35 lph flow rate. Up to this experiment, it is

not sure that only at 35 lph flow rate the slit width will be minimum for ever, So, in next step considering 1.3 $\mu\text{m/s}$ feed rate, the machining is carried out further with varying flow rate of electrolyte from 30 lph to 45 lph for selecting proper electrolyte flow rate that may give the minimum slit width.

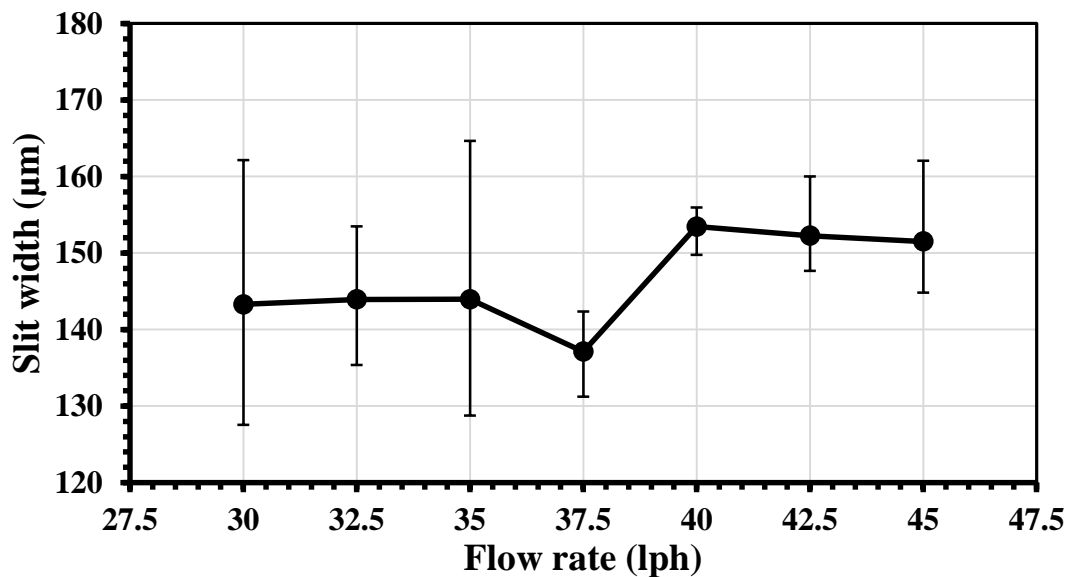


Fig. 5.5 Effect of flow rate on slit width

After analysing and measuring the micro slits with optical microscope, the calculated average slit width for each flow rate of electrolyte has been graphically represented as shown in Fig. 5.5. Here, the minimum slit is achieved, 137.13 μm at 37.5 lph flow rate and Fig. 5.6 shows the machining at that flow rate. This value has been considered in flow rate process parameter for final experiments of Multi-wire Electrochemical Micromachining (MWECEM) with Axial flushing criteria. Thereafter, the suitable process parameters are taken from all the previous experiments as shown in table 5.1 to establish a stable and good machining for final experimentations with varying feed rate.

Acquiring knowledge with some preliminary experiments on axial flushing, the stable parameter settings is established to analyse the effect of feed rate on slit width and accuracy of machining where 37.5 lph is considered as best flow rate in axial flushing. All these experiments are discussed below.

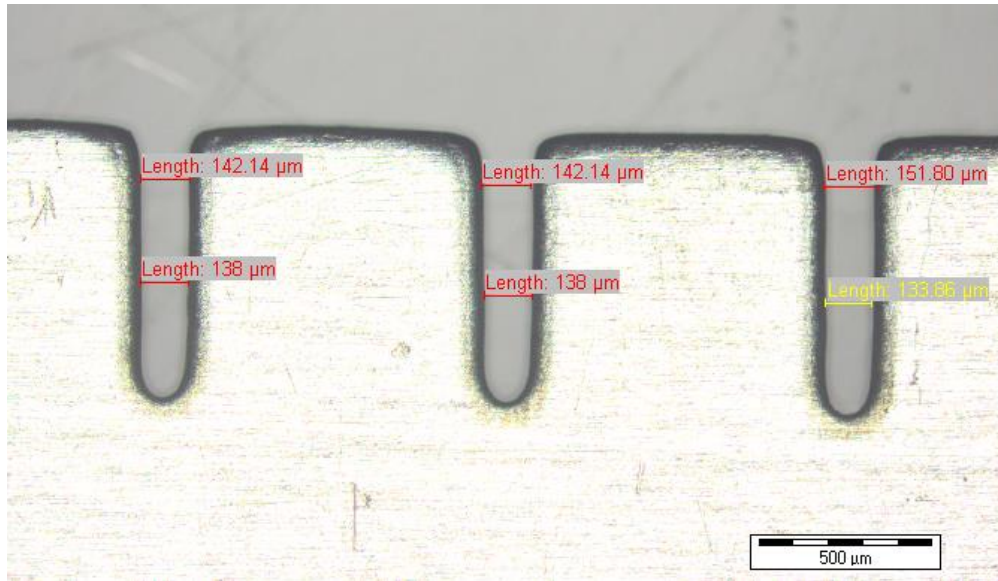


Fig. 5.6 Micro slits machining with three wire W electrodes having ϕ 50 μm , 12 V voltage, 12% duty ratio, 50 KHz frequency, 1.3 $\mu\text{m/s}$ feed, 0.1(M) H_2SO_4 concentration and 37.5 lph axial flushing flowrate

Experiment with 37.5 lph flow rate, 50 μm W wire, 12 V, 12 % duty ratio, 50 KHz applied frequency, 0.1 M H_2SO_4 solution and 0.5 $\mu\text{m/s}$ feed rate have showed good machining but high overcut is there. This high overcut occurs due to low feed travel which may facilitate the huge machining from the work piece.

Experiment with 37.5 LPH flow rate, 50 μm W wire, 12 V, 12 % duty ratio, 50 KHz applied frequency, 0.1 M H_2SO_4 solution and 0.7 $\mu\text{m/s}$ feed rate have showed the reduced overcut but not in acceptable range.

After experiment with 37.5 LPH flow rate, 50 μm W wire, 12 V, 12 % duty ratio, 50 KHz applied frequency, 0.1 M H_2SO_4 solution and 0.9 $\mu\text{m/s}$ feed rate to 2.1 $\mu\text{m/s}$ feed rate have showed the reduced slit width as the feed rate in increased, the dissolution rate is also reduced.

Later, experiment with 37.5 LPH flow rate, 50 μm W wire, 12 V, 12 % duty ratio, 50 KHz applied frequency, 0.1 M H_2SO_4 solution and 1.7 $\mu\text{m/s}$ feed have showed best machining along each wire that is shown in Fig. 5.7.

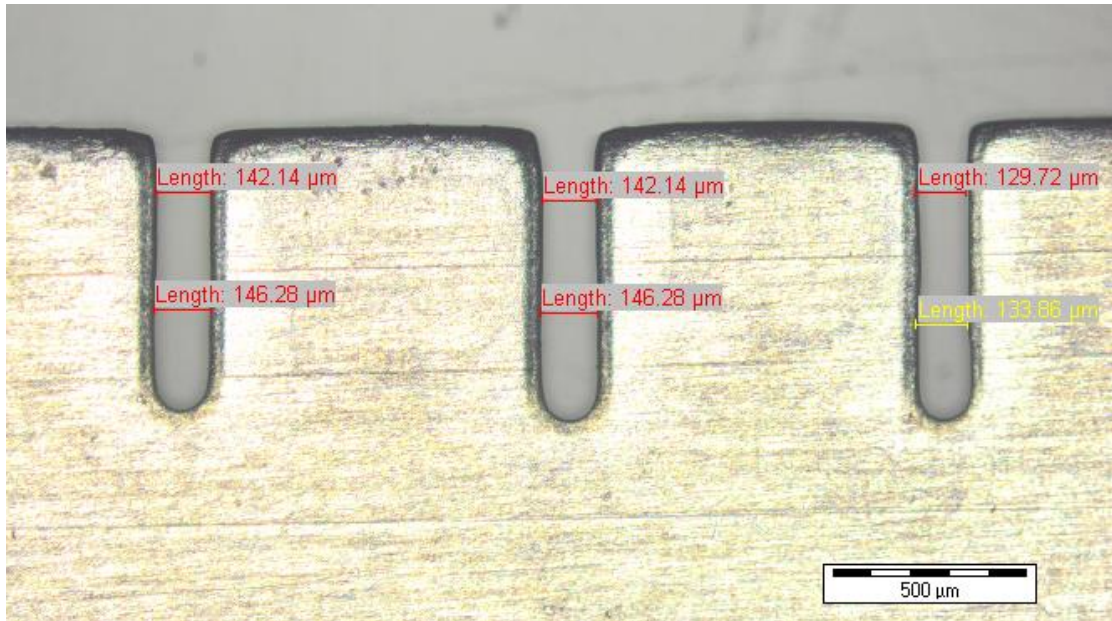


Fig. 5.7 Micro slits machining with three wires having ϕ 50 μm , 12 V voltage, 12% duty ratio, 50 KHz frequency, 0.1(M) H_2SO_4 concentration, 37.5 lph axial flushing flowrate and 1.7 $\mu\text{m/s}$ feed rate

But at 1.9 $\mu\text{m/s}$ feed rate the machining is well completed with minimum slit width of two ends electrodes and middle one is distorted with high overcut that signify the improper machining due to improper removal of sludge from machining zone with axial flushing at this high feed rate as a result other two ends electrodes get less current density and generate less micro slit width. Here among the three slits, one's width is large and other two are very small, this is due to the availability of unequal machining current along each wire.

Experiment with 37.5 LPH flow rate, 50 μm W wire, 12 V, 12 % duty ratio, 50 KHz applied frequency, 0.1 M H_2SO_4 solution and 2.1 $\mu\text{m/s}$ feed have showed negligible machining as shown in Fig. 5.8. Due to very high feed, anodic dissolution process is restricted in machining zone where proper electrolyte flushing is not successfully completed as at high feed slit width is also reduced. So, the flushing area is too narrow to pass out with sludge as a result short circuit occurs at the time of machining.

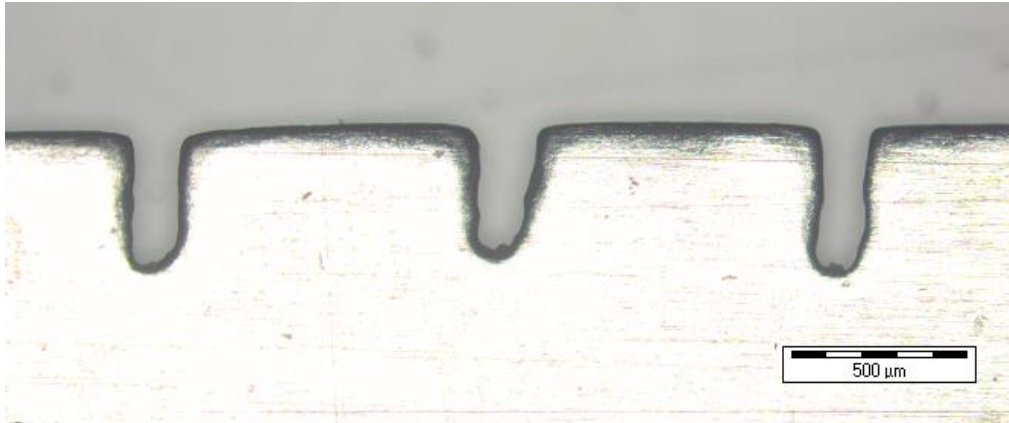


Fig. 5.8 Micro slits machining with three wire W electrodes having ϕ 50 μm , 12 V voltage, 12% duty ratio, 50 KHz frequency, 0.1(M) H_2SO_4 concentration, 37.5 lph axial flushing flowrate and 2.1 $\mu\text{m/s}$ feed rate

(i) Effect of feed rate on slit width

Figure 5.9 shows the influence of wire feed on average width of the fabricated micro slit. The graph has been plotted with the experimental results obtained at 0.5, 0.7, 0.9, 1.1, 1.3, 1.5, 1.7, 1.9 $\mu\text{m/s}$ feed rate by keeping the other parameters as fixed as, Flow rate, 37.5 lph; voltage, 12 V; Duty ratio, 12%; frequency, 50 KHz and concentration of electrolyte (H_2SO_4), 0.1 M. During experiments, the minimum experimental width of fabricated micro slit achieved is 137.13 μm whereas; the maximum width is 209.53 μm .

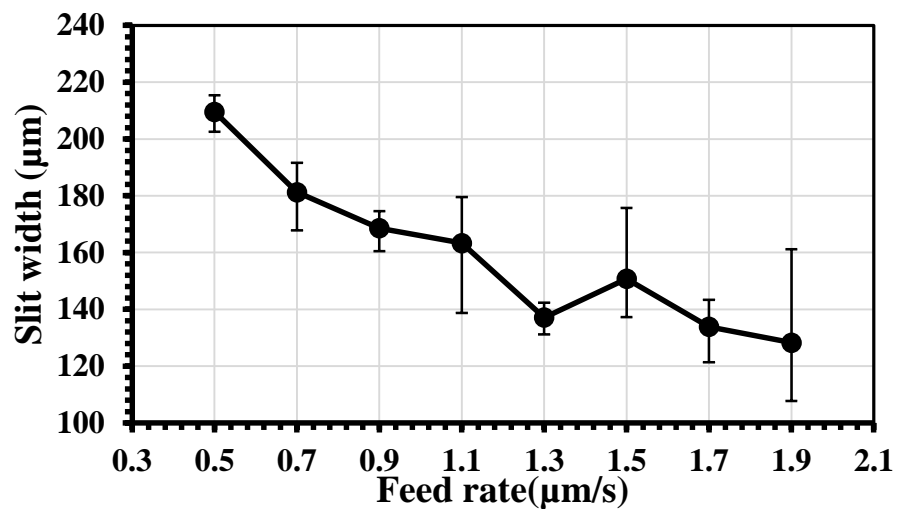


Fig. 5.9 The influence of feed on average width of the fabricated micro slit at 37.5 lph flow rate

(ii) Effect of feed rate on Accuracy of machining

After calculating the standard deviation of slit widths generated at 37.5 lph flow rate, with the experimental results obtained at 0.5, 0.7, 0.9, 1.1, 1.3, 1.5, 1.7, 1.9 $\mu\text{m/s}$ feed rate by keeping the other parameters as fixed as voltage, 12 V; Duty ratio, 12%; frequency, 50 KHz and concentration of electrolyte (H_2SO_4), 0.1 M, are plotted on graph as shown in Fig. 5.10 implies the influence of feed on accuracy of machining.

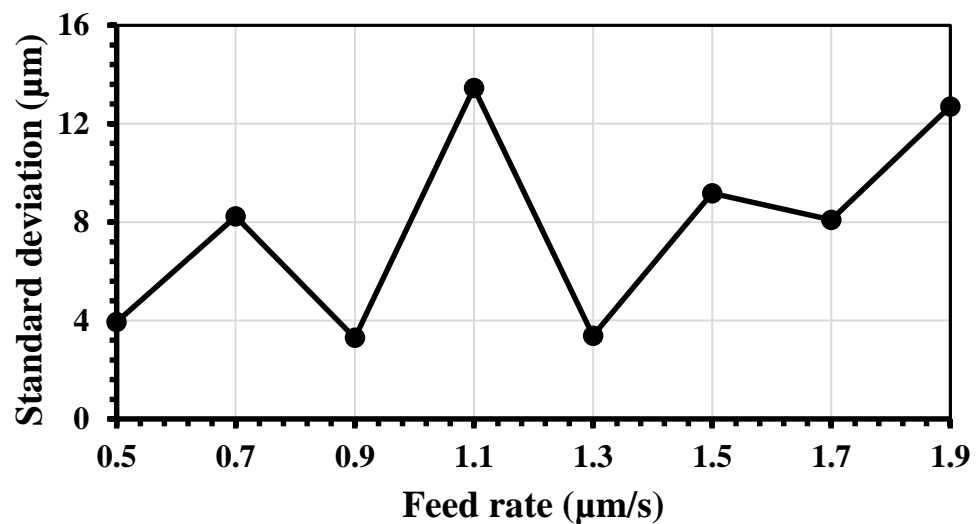


Fig. 5.10 Effect of feed rate on Accuracy of machining at 37.5 lph flow rate

The minimum standard deviation of fabricated micro slit achieved is 3.295 whereas; the maximum standard deviation is 13.45. The accuracy of generated micro slits in MWECM with axial flushing of 37.5 lph is approximately same at 0.5, 0.9, 1.3 $\mu\text{m/s}$ feed rate, but at 0.7 and 1.1 $\mu\text{m/s}$ feed rate the standard deviation abruptly increased.

5.3 Vibration assisted Multi-wire Electrochemical Micromachining (MWECM)

In place of axial flushing, PZT is used which generates axial vibration on multi wire electrodes to carry out the machining with MWECM setup. The PZT vibration will be helpful to mass transport in the machining zone. Experiments have been planned to study the effect of PZT during MWECM operation.

5.3.1 Planning for experimentation

Before starting machining with PZT, from the hysteresis curve of piezo system different vibration amplitudes are taken. At first, with high amplitude as 197.43 μm the machining is carried out at very low feed like 0.2, 0.35, 0.5 $\mu\text{m/s}$ where worse slit is generated and it is also continued for high feed as 0.9 $\mu\text{m/s}$ with same feature in slit. Then the experiments are done with reduced amplitude at 77.43 μm and 0.9 $\mu\text{m/s}$ feed rate which gives a better result. Thereafter with different amplitude from 17.43 to 97.43 μm are carried out to machining to check which one satisfy the minimum slit width and it is optimized at 57.43 μm vibration amplitude that is followed for rest of the machining where vibration frequency is always fixed to 60 Hz as it is the minimum value in the machining setup. The process parameters for the final experiments are shown in Table 5.2.

Table 5.2 Process parameters for carrying out final experiments with PZT

Process parameters	Values
Tungsten wire diameter, (μm)	50
Number of wire electrode	3
Stainless steel sheet thickness, (μm)	100
Initial inter electrode gap, (μm)	100
Voltage, (V)	12
Electrolyte	H ₂ SO ₄
Electrolyte concentration, (M)	0.1
Frequency, (KHz)	50
Duty ratio, (%)	12
Wire feed rate, ($\mu\text{m/sec}$)	0.5 – 1.5
Vibration amplitude, (μm)	57.43
Vibration frequency, (Hz)	60

5.3.2 Results and discussions

Initially, sets of primary experiments have been carried out taking tungsten wire of diameter 50 μm as cathode in three wire MWECEM setup and stainless steel (SS 304) sheet of thickness 100 μm as anode including PZT flushing technique. All the experiments have been conducted with 0.1 M H₂SO₄ electrolyte. At first PZT vibration amplitude is taken 197.43 μm from hysteresis curve and made some trial experiments at feed as like 0.2, 0.5, 0.9 $\mu\text{m/s}$ which shows bad machining due to the deposition of sludge on wires and bubbles are formed and stay on wires that comes in machining in

term of high overcut and at $0.9 \mu\text{m/s}$ feed it arises as worse machining with high fluctuating current where the work piece is distorted at slit ends as shown in Fig. 5.11. Thereafter, reducing the vibration amplitude to $77.43 \mu\text{m}$ at $0.9 \mu\text{m/s}$ feed the machining reaches a better and stable position with negligible sludge formed.

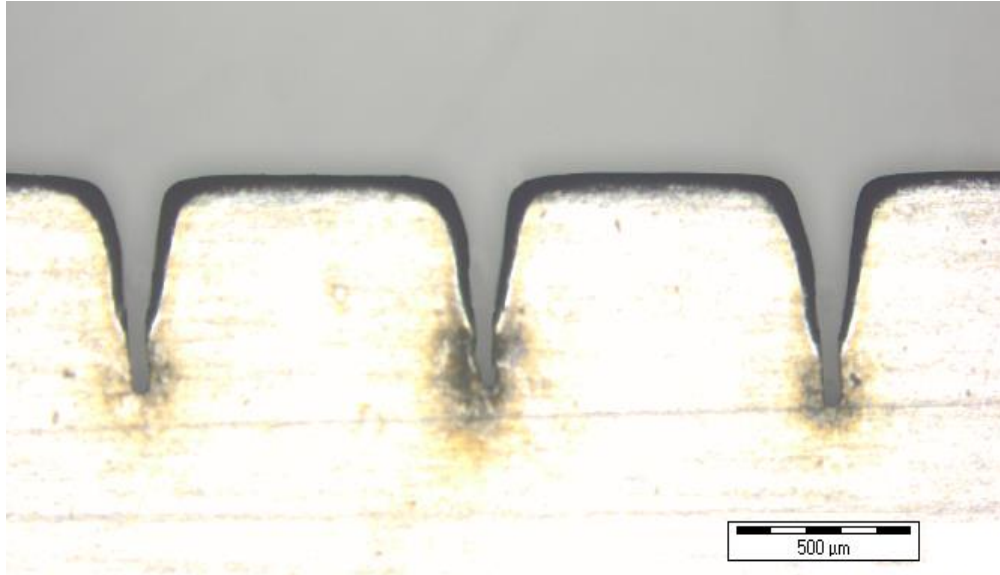


Fig. 5.11 Micro slits machining with three wire W electrodes having $\phi 50 \mu\text{m}$, 12 V voltage, 12% duty ratio, 50 KHz frequency, 0.1(M) H_2SO_4 concentration, $197.43 \mu\text{m}$ vibration amplitude, 60 Hz vibration frequency and $0.9 \mu\text{m/s}$ feed rate

After that, the feed rate is taken constant at $0.9 \mu\text{m/s}$, PZT flushing is observed at different vibration amplitude from $17.43 \mu\text{m}$ to $97.43 \mu\text{m}$ and for all the experiments IEG is taken as $100 \mu\text{m}$. After completing all this machining with three wire electrodes which are mounted in wire holding block with 1mm spacing in multi-wire electrochemical system, the average slit width is calculated from measured value of slit width of generated micro slits with optical microscope and are plotted them on graph as shown in Fig. 5.12. Here, at $97.43 \mu\text{m}$ vibration amplitude the machining is worse and not capable of machining in full length as planned. So, it is not shown in the graph.

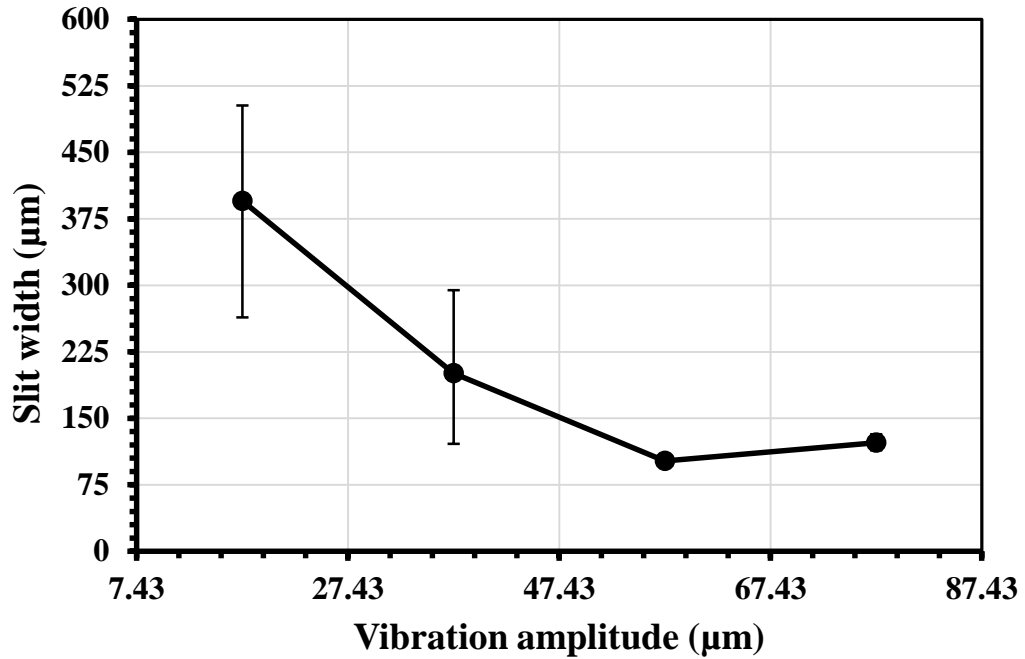


Fig. 5.12 Effect of PZT vibration amplitude on slit width

Here, the minimum slit is achieved at 57.43 μm vibration amplitude as shown in Fig. 5.12 and Fig. 13 and this value has been considered as process parameter for final experiments of Multi-wire Electrochemical Micromachining (MWECEM) with PZT flushing criteria. There after the suitable process parameters are taken from all the previous experiments as shown in table 5.2 to establish a stable and good machining for final experimentations with varying feed rate from 0.5 $\mu\text{m/s}$ to 1.5 $\mu\text{m/s}$. All the experiments are obtained to analyse the effect of feed rate on slit width and accuracy of machining where 57.43 μm is considered as best vibration amplitude in PZT flushing. All these experiments are discussed below.

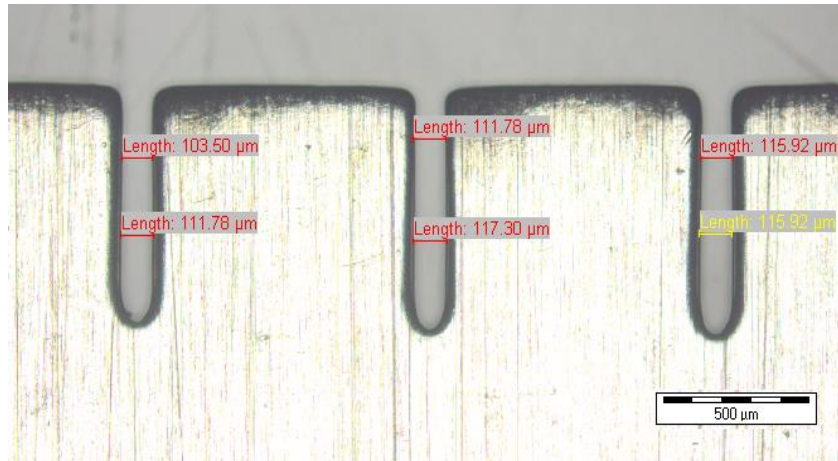


Fig. 5.13 Micro slits machining with three wire W electrodes having ϕ 50 μm , 12 V voltage, 12% duty ratio, 50 KHz frequency, 0.1(M) H_2SO_4 concentration, 57.43 μm vibration amplitude, 60 Hz vibration frequency and 0.9 $\mu\text{m/s}$ feed rate

Experiment with 57.43 μm vibration amplitude, 60 Hz vibration frequency, 50 μm W wire, 12 V, 12 % duty ratio, 50 KHz applied frequency, 0.1 M H_2SO_4 solution and 0.5 $\mu\text{m/s}$ feed rate have showed good machining but high overcut is there. This high overcut occurs due to low feed travel which may facilitate the huge machining from the work piece and also the effect of sludge deposition on wires, bubbles formation that are stayed in wires.

Experiment with 57.43 μm vibration amplitude, 60 Hz vibration frequency, 50 μm W wire, 12 V, 12 % duty ratio, 50 KHz applied frequency, 0.1 M H_2SO_4 solution and 0.7 $\mu\text{m/s}$ feed rate have showed the reduced overcut but not in acceptable range. Here, micro spark is generated at the time of machining and sludge is deposited on the middle wire of three.

Later, experiment with 57.43 μm vibration amplitude, 60 Hz vibration frequency, 50 μm W wire, 12 V, 12 % duty ratio, 50 KHz applied frequency, 0.1 M H_2SO_4 solution and 0.9 to 1.3 $\mu\text{m/s}$ feed have showed good machining with reduced slit width as the feed rate in increased, the dissolution rate is also reduced. Here, no visible sludge is found, but micro spark occurs in each case and at 1.3 $\mu\text{m/s}$ feed minimum slit width is achieved as shown in Fig. 5.14.

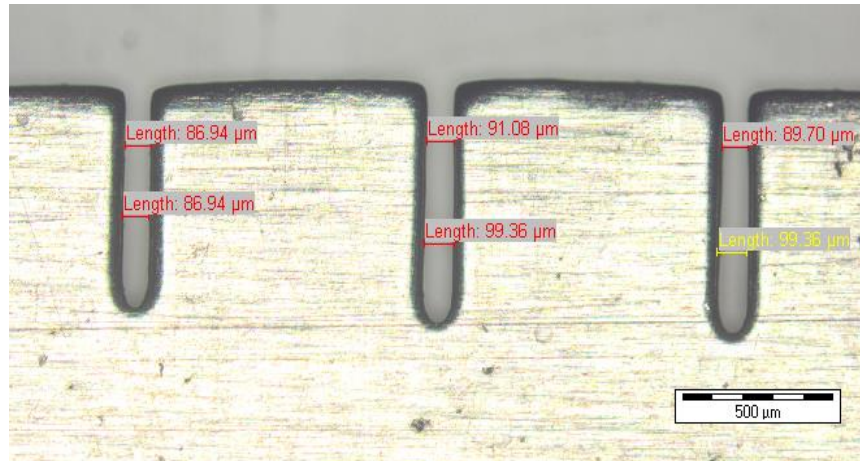


Fig. 5.14 Micro slits machining with three wire W electrodes having ϕ 50 μm , 12 V voltage, 12% duty ratio, 50 KHz frequency, 0.1(M) H_2SO_4 concentration, 57.43 μm vibration amplitude, 60 Hz vibration frequency and 1.3 $\mu\text{m/s}$ feed rate

After, experiment with 57.43 μm vibration amplitude, 60 Hz vibration frequency, 50 μm W wire, 12 V, 12 % duty ratio, 50 KHz applied frequency, 0.1 M H_2SO_4 solution and 1.5 $\mu\text{m/s}$ feed have showed worse and incomplete machining. Due to very high feed, anodic dissolution process is restricted in machining zone where proper electrolyte flushing is not successfully completed as at high feed slit width is also reduced. So, the flushing area is too narrow to pass out with sludge as a result short circuit occurs at the time of machining.

(i) Effect of feed rate on slit width

Figure 5.15 shows the influence of feed on average width of the fabricated micro slit. The graph has been plotted with the experimental results obtained at 0.5, 0.7, 0.9, 1.1, 1.3 $\mu\text{m/s}$ feed rate by keeping the other parameters as fixed as, 57.43 μm vibration amplitude, 60 Hz vibration frequency, 50 μm W wire, 12 V applied voltage, 12 % duty ratio, 50 KHz applied frequency, 0.1 M H_2SO_4 solution. During experiments, the minimum experimental width of fabricated micro slit achieved is 87.275 μm whereas; the maximum width is 273.041 μm .

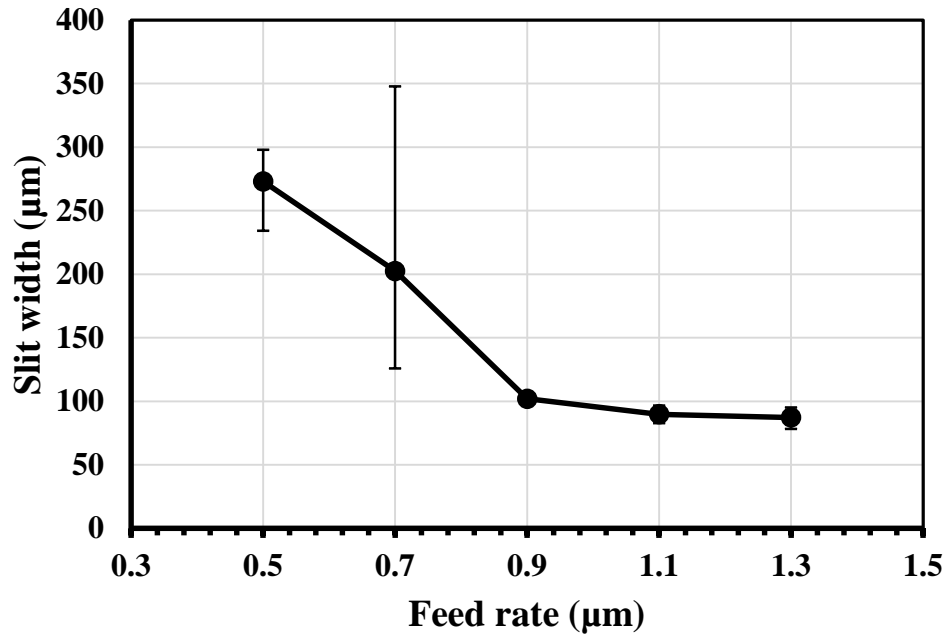


Fig. 5.15 The influence of feed on average width of the fabricated micro slit at 57.43 μm PZT vibration amplitude, 60 Hz vibration frequency

(ii) Effect of feed rate on Accuracy of machining

After calculating the standard deviation of slit widths generated at 57.43 μm vibration amplitude, with the experimental results obtained at 0.5, 0.7, 0.9, 1.1, 1.3 $\mu\text{m/s}$ feed rate by keeping the other parameters as fixed as voltage, 12 V; Duty ratio, 12%; frequency, 50 KHz and concentration of electrolyte (H_2SO_4), 0.1 M, are plotted on graph as shown in Fig. 5.16 implies the influence of feed on accuracy of machining.

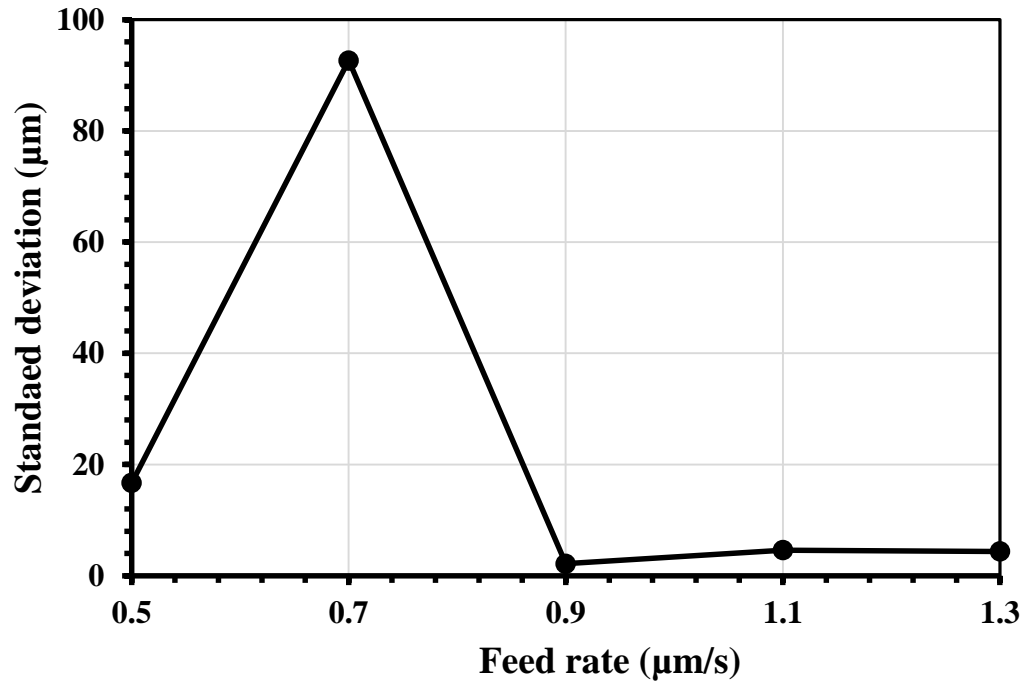


Fig. 5.16 Effect of feed rate on Accuracy / Homogeneity of machining at 57.43 µm PZT vibration amplitude, 60 Hz vibration frequency

The minimum standard deviation of fabricated micro slit achieved is 3.295 whereas; the maximum standard deviation is 13.45. The accuracy of generated micro slits in MWECM with PZT flushing 57.43 µm vibration amplitude is best at 0.9 µm/s feed rate, but at 1.1 and 1.3 µm/s feed rate the standard deviation almost same and better.

5.4 Combination of axial flushing and vibration assisted Multi-wire Electrochemical Micromachining (MWECM)

Another flushing strategy is introduced here with axial flushing and vibration with the help of PZT combined in Multi-wire Electrochemical Micromachining (MWECM). Combined effect of both during machining is studied to achieved better flushing criteria during MWECM operation.

5.4.1 Planning for experimentation

After taking out previous experiments along with two different flushing technique in Multi-wire Electrochemical Micromachining (MWECEM), best flushing parameters are combined here to achieve a stable and best machining ever. For that, 37.5 lph flow rate of axial flushing and 57.43 μm vibration amplitude of PZT are considered as a new process parameter in this experimentation with this combined flushing type. The process parameters for carrying out the final experiments with axial flushing and PZT are shown in Table 5.3.

Table 5.3 Process parameters for carrying out final experiments with Axial flushing and PZT

Process parameters	Values
Tungsten wire diameter, (μm)	50
Number of wire electrode	3
Stainless steel sheet thickness, (μm)	100
Initial inter electrode gap, (μm)	100
Voltage, (V)	12
Electrolyte	H ₂ SO ₄
Electrolyte concentration, (M)	0.1
Frequency, (KHz)	50
Duty ratio, (%)	12
Wire feed rate, ($\mu\text{m}/\text{sec}$)	0.5 – 1.5
Electrolyte Flow rate, (lph)	37.5
Vibration amplitude, (μm)	57.43
Vibration frequency, (Hz)	60

5.4.2 Results and discussions

With the suitable process parameters taken from all the previous experiments as shown in table 5.3 a stable and good machining for final experimentations with varying feed rate from 0.5 $\mu\text{m}/\text{s}$ to 1.9 $\mu\text{m}/\text{s}$ is established where Axial flushing and PZT combined. All the experiments are obtained to analyse the effect of feed rate on slit width and accuracy of machining where 37.5 lph is considered as best axial flushing flow rate and 57.43 μm is considered as best vibration amplitude in PZT flushing. All these experiments are discussed below.

Experiment with 37.5 lph flow rate, 57.43 μm vibration amplitude, 60 Hz vibration frequency, 50 μm W wire, 12 V, 12 % duty ratio, 50 KHz applied frequency, 0.1 M H₂SO₄ solution and 0.5 $\mu\text{m}/\text{s}$ feed rate have showed good machining but high overcut is there. This high overcut occurs due to low feed travel which may facilitate the huge machining from the work piece and also the effect of wire vibration.

Experiment with 37.5 LPH flow rate, 57.43 μm vibration amplitude, 60 Hz vibration frequency, 50 μm W wire, 12 V, 12 % duty ratio, 50 KHz applied frequency, 0.1 M H_2SO_4 solution and 0.7 to 1.7 $\mu\text{m}/\text{s}$ feed rate have showed the reduced overcut in gradual manner. Here, micro spark is not generated at the time of machining and sludge is not deposited on the wires and 1.7 $\mu\text{m}/\text{s}$ feed rate have minimum slit width of 87.273 μm as shown in Fig. 5.17.

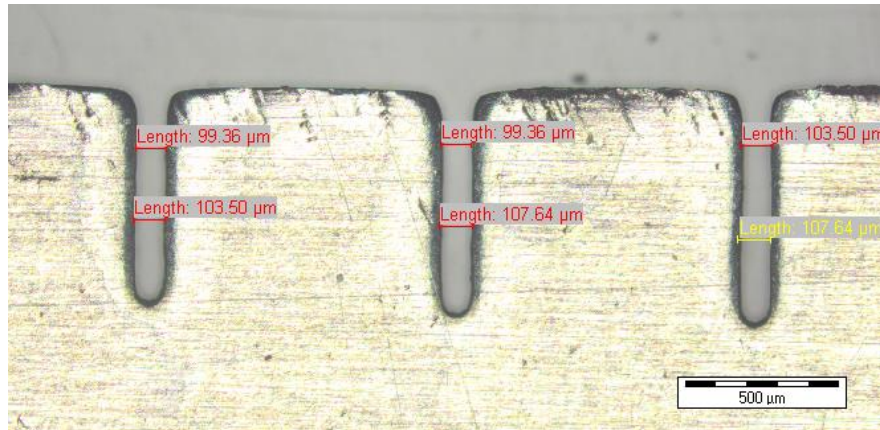


Fig. 5.17 Micro slits machining with three wire W electrodes having ϕ 50 μm , 12 V voltage, 12% duty ratio, 50 KHz frequency, 0.1(M) H_2SO_4 concentration, 37.5 lph axial flushing flowrate, 57.43 μm vibration amplitude, 60 Hz vibration frequency and 1.7 $\mu\text{m}/\text{s}$ feed rate

Later, experiment with 37.5 lph flow rate, 57.43 μm vibration amplitude, 60 Hz vibration frequency, 50 μm W wire, 12 V, 12 % duty ratio, 50 KHz applied frequency, 0.1 M H_2SO_4 solution and 1.9 $\mu\text{m}/\text{s}$ feed rate have showed worse and negligible machining. Due to very high feed, anodic dissolution process is restricted in machining zone where proper electrolyte flushing is not successfully completed as at high feed, slit width is also reduced. So, the flushing area is too narrow to pass out with sludge, as a result short circuit occurs at the time of machining.

(i) Effect of feed rate on slit width

Figure 5.18 shows the influence of feed on average width of the fabricated micro slit. The graph has been plotted with the experimental results obtained at 0.5, 0.7, 0.9, 1.1, 1.3, 1.5, 1.7 $\mu\text{m}/\text{s}$ feed rate by keeping the other parameters as fixed as, 37.5 lph flow rate , 57.43 μm vibration amplitude, 60 Hz vibration

frequency, 50 μm W wire, 12 V applied voltage, 12 % duty ratio, 50 KHz applied frequency, 0.1 M H_2SO_4 solution. During experiments, the minimum experimental width of fabricated micro slit achieved is 90.62 μm whereas; the maximum width is 251.746 μm .

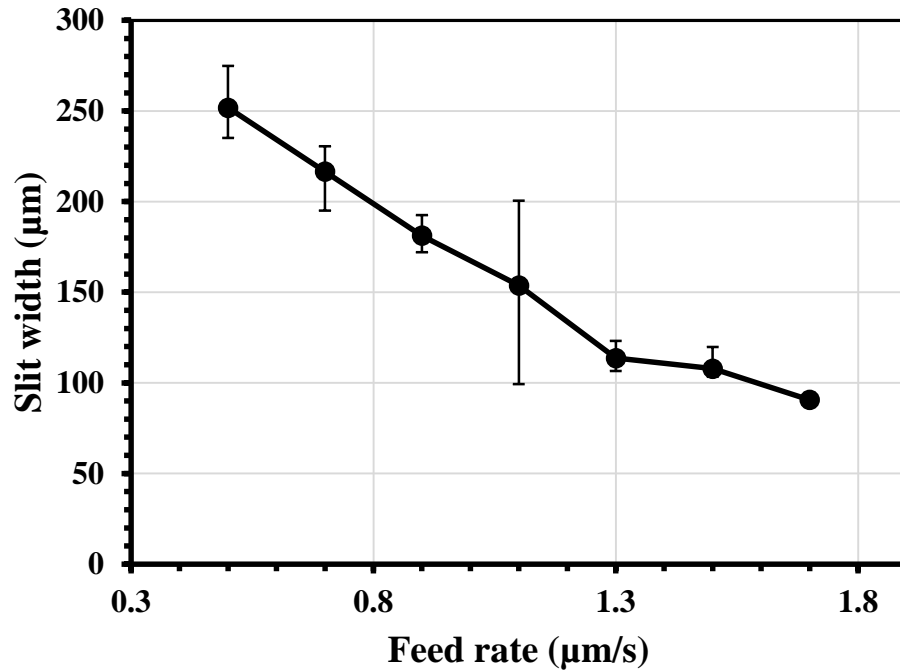


Fig. 5.18 The influence of feed on average width of the fabricated micro slit at 37.5 lph flow rate, 57.43 μm PZT vibration amplitude, 60 Hz vibration frequency

(i) Effect of feed rate on accuracy of machining

After calculating the standard deviation of slit widths generated at 37.5 lph flow rate, 57.43 μm vibration amplitude, with the experimental results obtained at 0.5, 0.7, 0.9, 1.1, 1.3, 1.5, 1.7 $\mu\text{m/s}$ feed rate by keeping the other parameters as fixed as voltage, 12 V; Duty ratio, 12%; frequency, 50 KHz and concentration of electrolyte (H_2SO_4), 0.1 M, are plotted on graph as shown in Fig. 5.19 which implies the influence of wire feed on accuracy of machining.

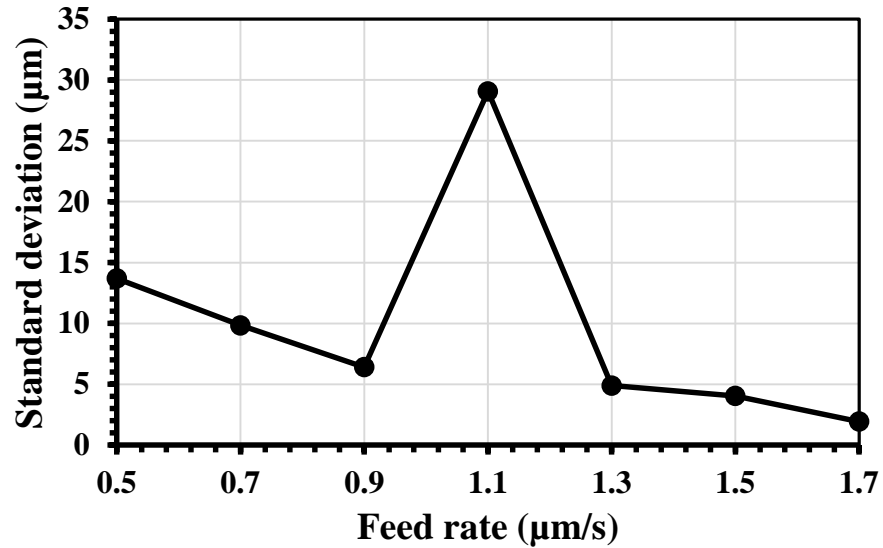


Fig. 5.19 Effect of feed rate on Accuracy / Homogeneity of machining at 37.5 lph flow rate, 57.43 µm PZT vibration amplitude, 60 Hz vibration frequency

The minimum standard deviation of fabricated micro slit achieved is 1.94, whereas; the maximum standard deviation is 29.066. The accuracy of generated micro slits in MWECM with axial flushing and PZT combined is best at 1.7 µm/s feed rate, but at 1.1 µm/s feed rate the standard deviation almost is too high.

5.5 Comparison among different flushing strategies incorporated with Multi-wire Electrochemical Micromachining (MWECM)

In WECM, the conductivity of electrolyte in the IEG is vividly dependent on the amount of electrolysis products, gas bubbles and temperature etc. However, the temperature in machining area having minimal effect which can be neglected. This phenomenon is also applicable to MWECM, where without taking proper mass transfer techniques or better electrolyte flushing strategies, the volume of electrolysis product in the IEG increases, resulting fluctuation of actual machining gap which influences short circuiting and producing micro sparks that deteriorate the stability and the accuracy of micro features. Here, in the following discussion a basic comparison among previously mentioned three different flushing criteria is focused to get a best electrolyte flushing technique that can help to reach desired target of generating high quality micro features with MWECM process.

As shown in Fig. 5.20, the experimental data of all three electrolyte flushing strategy regarding average slit width with respect to different feed rate implies that PZT vibration assisted MWECM process and combination of axial flushing and PZT vibration assisted MWECM has successfully been run in the range of 0.5 to 1.3 $\mu\text{m/s}$ and 0.5 to 1.7 $\mu\text{m/s}$ wire feed rate respectively. But, axial flushing assisted MWECM process has successfully been run in the range of 0.5 to 1.9 $\mu\text{m/s}$ wire feed rate, that is the maximum achievable range of wire feed rate. The minimum slit width is 87.27 μm , achieved in axial vibration using PZT assisted flushing, where as in axial electrolyte flushing the value of slit width can't reach to the desired value. In lieu of using the above mentioned two techniques combining both gives moderate width, 90.62 μm that can reach at high feed of 1.7 $\mu\text{m/s}$. It is also concluded that these three flushing techniques individually have a limitation in maximum acceptable feed rate to continue proper machining. Here, it is clear to make decision about the machining that at high feed rate where only PZT can't continue machining due to improper flushing and coming back of sludge in machining gap due to lack of dissolution time at high feed rate, addition of axial flow of electrolyte make it possible to generate micro slit that is more accurate machining compare to the rests as shown in Fig. 5.19.

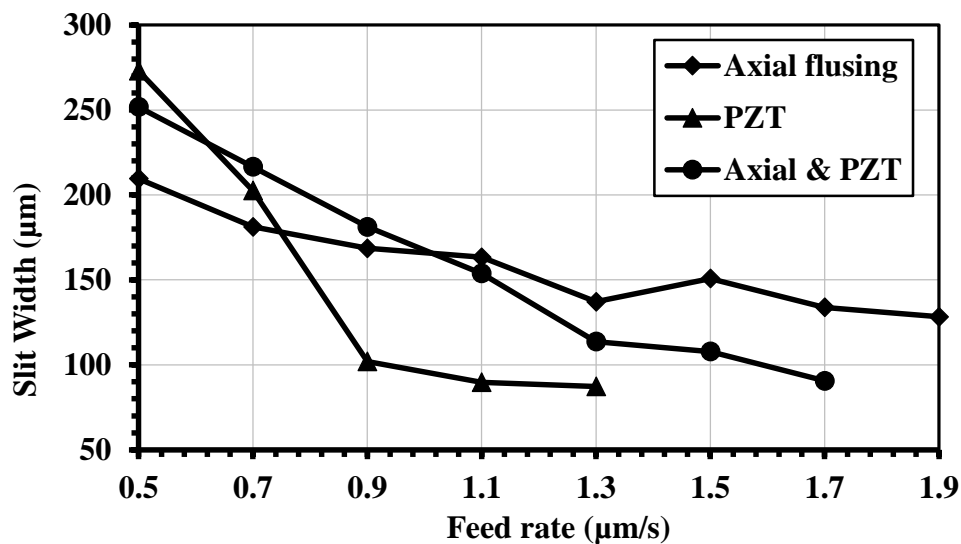


Fig. 5.20 Comparison among three different flushing strategies related to slit width at different feed rate in MWECM process

Accuracy of machining in MWECM deteriorates if micro sparks occur, clogging of bubbles and sludge generate on wire and in machining gap during machining. This

challenge is taken care of with three different flushing strategy, where in term of comparison only combined axial flow and axial vibration of multi wires electrodes fulfil the objective of improving accuracy as shown in Fig. 5.21. In case of using PZT vibration in wires, micro sparks occur at high feed rate that also deteriorate the accuracy of machining though it can generate minimum slit width and on the other hand, axial flow of electrolyte generates improper accuracy due to instability of wire electrodes due to impingement of electrolyte flow on the wires during machining. The minimum standard deviation is 1.94 μm , achieved with axial and PZT combined flushing at 1.9 $\mu\text{m/s}$ feed rate.

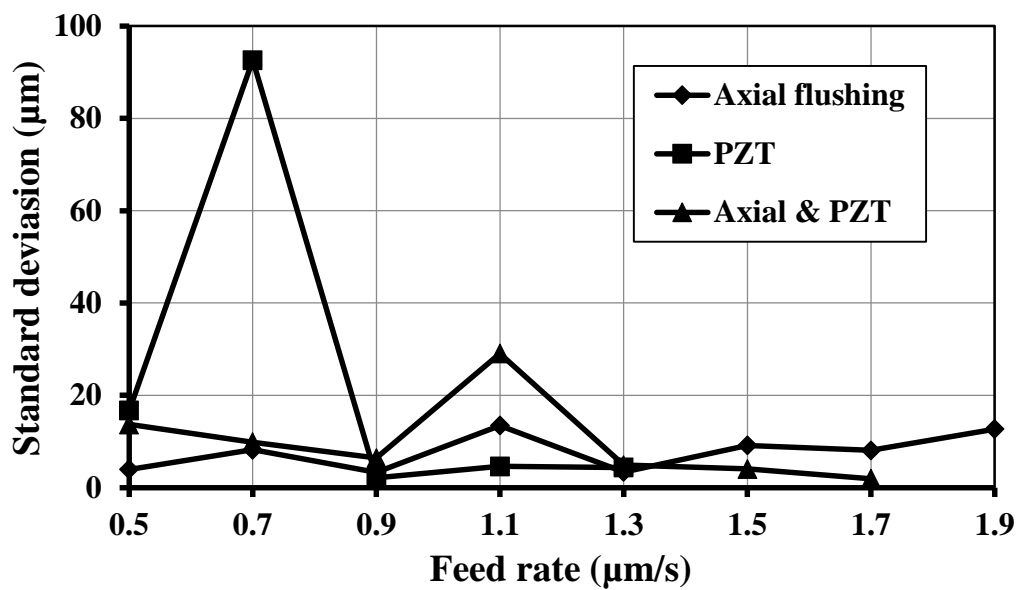


Fig. 5.21 Comparison among three different flushing criteria related to machining accuracy at different feed rate in MWECEM process

5.6 Analysis and validation of mathematical models of slit width

To get more stability of the MWECEM process, the mathematical model that have been developed are theoretically analysed and validated with practical results in this study.

To verify the developed mathematical model with practical results and to carry out theoretical analysis, both theoretical and experimental widths of the fabricated micro slits have been graphically represented with three different flushing techniques where other parameters have been kept constant at voltage, 12 V Duty ratio, 12%; frequency, 50 KHz and concentration of electrolyte (H_2SO_4), 0.1 M. During calculation of

theoretical width of the micro slit, values of different parameters are considered as listed in Table 5.4.

Table 5.4 Values of different parameters considered during calculation of theoretical width

Different parameters	Values
ρ , (ohm.cm)	73×10^{-6}
C_d , (Farad)	114.2×10^{-6}
δ_{fg} , (cm)	0.01
e_a , (gm/mol/coloumb)	2.8935×10^{-4}
K_e , (S/cm)	299.5×10^{-6}
ρ_a , (gm/cc)	8

During validation all the theoretical calculations are obtained from the Eq. no. 25 at different feed rate that are required to facilitate machining with three different flushing criteria. From this validation a clear concept of micro feature fabrication technique in MWECCM will be obtained.

As shown in Fig. 5.22, the value of theoretical slit width and other results obtained from experiments are plotted simultaneously and here it represents the more precisely validated flushing technique is PZT in the range of wire feed rate from 0.9 to 1.3 $\mu\text{m/s}$. But, from the other two flushing types combination of axial flushing and PZT vibration make a very close validation at 1.7 $\mu\text{m/s}$ wire feed rate.

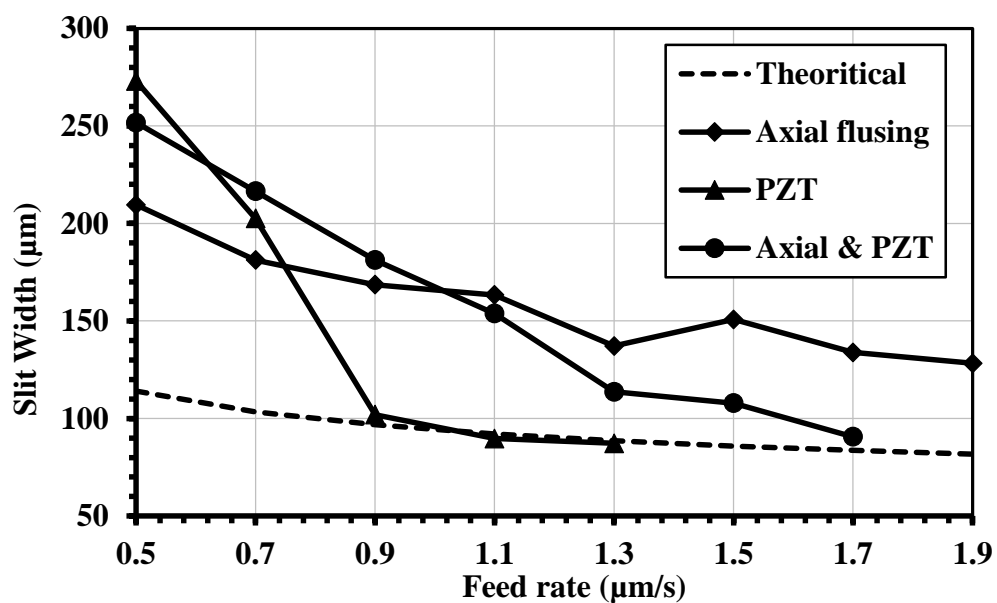


Fig. 5.22 Validation of mathematical model of slit width with different flushing techniques.

Calculated value of theoretical slit width at 0.5, 0.7, 0.9, 1.1, 1.3, 1.5, 1.7 and 1.9 $\mu\text{m/s}$ wire feed rate are 113.98, 103.4, 96.77, 92.12, 88.62, 85.87, 83.64 and 81.77 μm respectively. It is clearly visible that from 0.9 to 1.3 $\mu\text{m/s}$ wire feed, PZT has great influence to generate micro slit, where as other techniques only carry out the trend with respect to theoretical value. This prediction comes close at high feed only; at low range of wire feed it deteriorates abruptly.

5.7 Fabrication of micro features using Multi-wire Electrochemical Machining (MWECM) process

Multiple micro slit structure has been fabricated with three $\text{\O} 50 \mu\text{m}$ tungsten wire system, spacing 1000 μm as shown in Fig. 5.23, where average width of micro slits is 89.71 μm . This machining is completed with the parameter of applied voltage 12V; duty ratio 12%; wire feed rate 1.1 $\mu\text{m/s}$; 50 KHz applied frequency; 0.1 M H_2SO_4 solution; 57.43 μm vibration amplitude, 60 Hz vibration frequency. The machining is repeated on a new work area after completion of one machining stage, further movement of multiple wire holding block along X axis for 1 mm is made to start second machining stage for fabricating multiple micro slits on SS304 work specimen simultaneously.

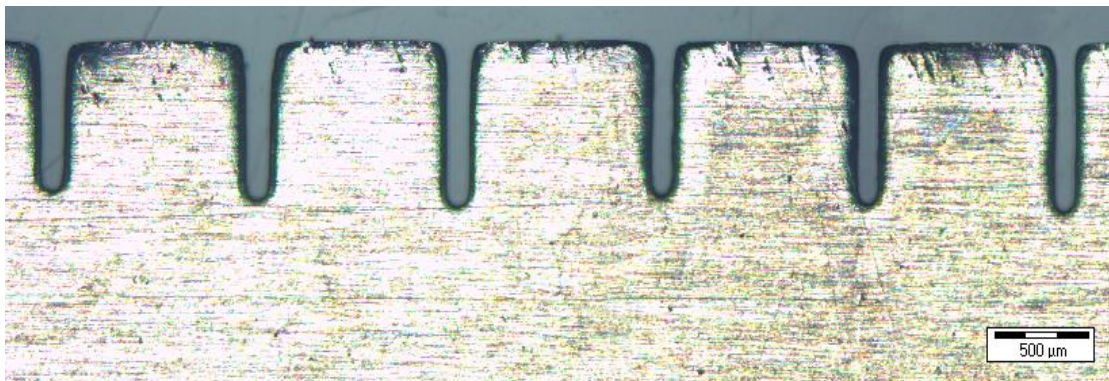


Fig. 5.23 Multiple micro slits fabricated with 57.43 μm PZT vibration amplitude, 1.1 $\mu\text{m/s}$ wire feed rate

With the same MWECM setup another approach is taken to fabricate some complex shaped micro features where two wires are mounted on wire holding device, spacing 2 mm in place of three wire in the previous system. Here, spiral shaped feature is

generated as shown in Fig. 5.24, with some changed parameter settings, as follows, 11 V applied voltage is used in place of 12 V, as number of wire electrodes change from three to two and 37.5 lph axial flushing flow rate with 1.3 $\mu\text{m/s}$ feed rate, keeping rest of the other parameter same.

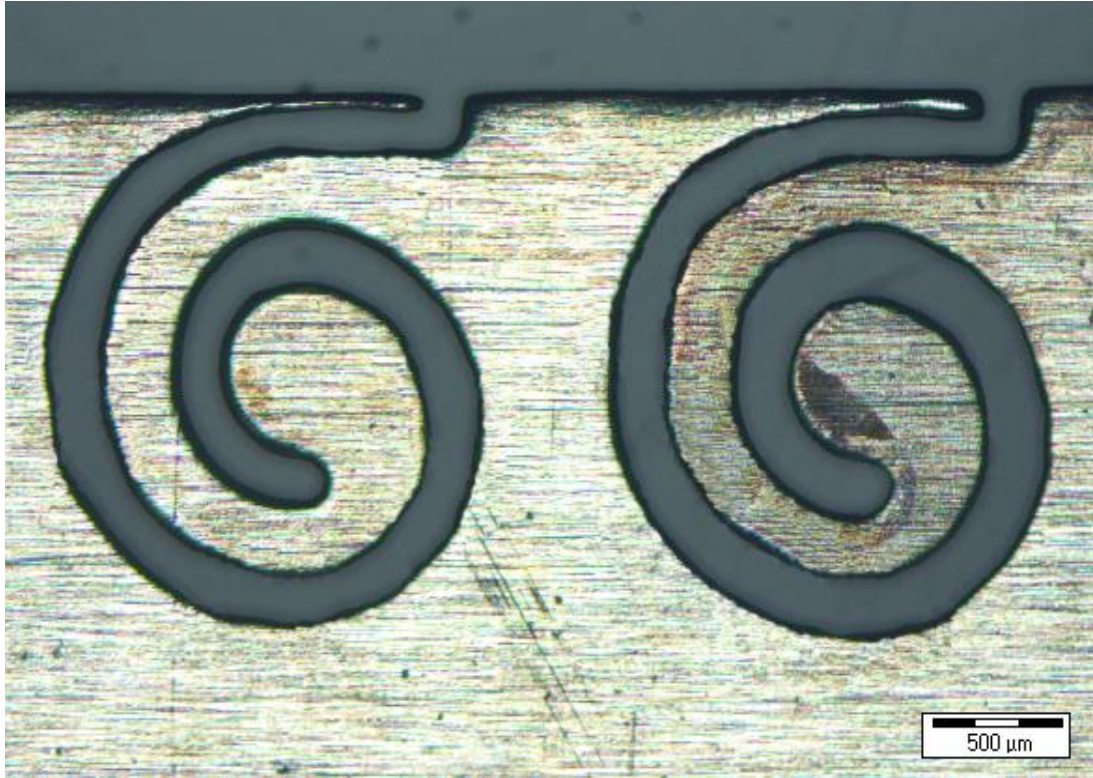


Fig. 5.24 Spiral shaped complex feature fabricated with two wire system, 11 V applied voltage, 37.5 lph axial flushing flow rate, 1.3 $\mu\text{m/s}$ feed rate

6. GENERAL CONCLUSIONS

This research work is focussed upon the advancement of the WECM process in terms of Multi-wire Electrochemical Micromachining (MWECM) which has been achieved successfully. This significant research work has been carried out theoretically as well as experimentally on different aspects of Electrolyte flushing strategy in MWECM process. The general conclusions that can be drawn from this research work are listed below:

- (i) A multi-wire electrochemical micromachining setup has successfully been developed, where three 50 μm diameter tungsten wire electrodes are mounted with 1mm inter electrode spacing and that can fulfil the demand of generating micro slits on SS304 specimen with high accuracy during MWECM operation.
- (ii) A mathematical model for MWECM considering double layer charging theory has been developed for predicting slit width. Width of the micro slits that are to be fabricated for particular parameter settings of MWECM considering three different electrolyte flushing strategies with respect to varying wire feed rate. The developed model is successfully validated with the experimental results.
- (iii) With the help of axial flushing technique, experiments on multi-wire electrochemical machining have been done with varying feed rate range of 0.5 $\mu\text{m/s}$ to 2.1 $\mu\text{m/s}$ and keeping the other parameters as fixed as, flow rate, 37.5 lph; voltage, 12 V; Duty ratio, 12%; frequency, 50 KHz and concentration of electrolyte (H_2SO_4), 0.1 M, the maximum average width is 209.53 μm whereas the minimum average width of fabricated micro slit achieved is 137.13 μm .
- (iv) When the experiments with PZT vibration having vibration amplitude 57.43 μm and vibration frequency 60 Hz have been completed successfully; the maximum average width is 273.041 μm whereas, the minimum average experimental width of fabricated micro slit achieved is 87.275 μm , keeping

the other parameters as fixed as axial flushing and here also the changes of slit width and accuracy have been varied with feed rate range of 0.5 $\mu\text{m/s}$ to 1.3 $\mu\text{m/s}$.

- (v) Experiments with Axial flushing at 37.5 lph combined with PZT vibration with amplitude 57.43 μm ; frequency 60 Hz generated 251.746 μm maximum slit width and 90.62 μm minimum average experimental slit width of fabricated micro slits at varying feed rate ranges from 0.5 $\mu\text{m/s}$ to 1.7 $\mu\text{m/s}$, keeping other parameters fixed as in the case of the other two flushing strategies. The best parameter of axial flushing and PZT vibration is found more accurate during MWECEM operation.
- (vi) A comparison among these three different electrolyte flushing techniques have been carried out during MWECEM operation. The comparison with respect to the experimental results on slit width and accuracy of machining, established the fact that combination of axial flushing and PZT vibration technique is more effective for MWECEM operation.
- (vii) The shape and accuracy of generated multiple microslits structure and complex type micro features on SS304 represent the capability of the developed MWECEM setup for successful fabrication of complex microfeatures.

Multi-wires Electrochemical Machining (MWECEM) has very high potential for application in the aeronautics, automobile, electronic and biomedical industries. MWECEM can fabricate micro features from wide ranges of work materials. As in MWECEM process, the material is removed by electrochemical reactions, any adverse thermal effect is absent with generation of very high surface quality. In this process wire is not eroded and can be reused and having less diameter and it is environment friendly process. This reasons can establish the MWECEM process superior to Wire-EDM process in mass production. High aspect ratio complex shaped micro structures

with high productivity which are needed for MEMS applications can be fabricated employing MWECEM process.

Still Multi-wires Electrochemical Machining is not yet fully developed process for utilisation in the industrial applications. Extensive research work in different aspects of MWECEM is still needed so that MWECEM can be used as a commercial process in different industries for fabrication of micro features with high accuracy and quality.

Future scopes of work

To continue the next level of advancement of Multi-wire Electrochemical Machining (MWECEM), in-depth research are still needed for minimizing difficulties involved with it and to make it fully commercialized process. The further scopes of research in MWECEM are listed below.

- (i) Micro slits and micro features with same dimensions are generated using MWECEM process. However, micro slits or micro features having different width can also be generated with the help of varying diameter of employed wire at a time with same MWECEM setup.
- (ii) Effect of wire feed rate is to be consider during the mathematical modelling of the slit width while other process parameters are kept constant. Considering the same mathematical modelling, effects of other process parameters can also be studied.
- (iii) Micro slits having different dimension, which can be fabricated by controlling the machining current through each wire electrode during MWECEM.

References

1. Yong-Bin Zeng, Qia Yu, Shao-Hua Wang, and Di Zhu, "Enhancement of mass transport in micro wire electrochemical machining". *CIRP Annals - Manufacturing Technology*, 2012. 61: 195-198.
2. Kun Xu, Yongbin Zeng, Peng Li, and Di Zhu, "Study of surface roughness in wire electrochemical micro machining". *Journal of Materials Processing Technology*, 2015. 222: 103-109.
3. Qu Ningsong, Fang Xiaolong, Li Wei, Zeng Yongbin, and Zhu Di, "Wire electrochemical machining with axial electrolyte flushing for titanium alloy". *Chinese Journal of Aeronautics*, 2013. 26(1): 224-229.
4. Kun Xu, Yongbin Zeng, Peng Li, and Di Zhu, "Vibration assisted wire electrochemical micro machining of array micro tools". *Precision Engineering*, 2017. 47: 487-497.
5. Lingchao Meng, Yongbin Zeng, Xiaolong Fang, and Di Zhu, "Micropatterning of Ni-based metallic glass by pulsed wire electrochemical micro machining". *Intermetallics*, 2017. 81: 16-25.
6. Haidong He, Yongbin Zeng, Yangyang Yao, and Ningsong Qu, "Improving machining efficiency in wire electrochemical micromachining of array microstructures using axial vibration-assisted multi-wire electrodes". *Journal of Manufacturing Processes*, 2017. 25: 452-460.
7. Fang Xiaolong, Zhang Pengfei, Zeng Yongbin, Qu Ningsong, and Zhu Di, "Enhancement of performance of wire electrochemical micromachining using a rotary helical electrode". *Journal of Materials Processing Technology*, 2016. 227: 129-137.
8. Haidong He, Yongbin Zeng, and Ningsong Qu, "An investigation into wire electrochemical micro machining of pure tungsten". *Precision Engineering*, 2016. 45: 285-291.

9. Yongbin Zeng, Huajian Ji, Xiaolong Fang, Yufeng Wang, and Ningsong Qu "Analysis and Reduction of Stray-Current Attack in Reciprocated Traveling Wire Electrochemical Machining". *Advances in Mechanical Engineering*. 2014. DOI: 10.1155/2014/505932.
10. Kun Xu, Yongbin Zeng, Peng Li, Xiaolong Fang, and Di Zhu, "Effect of wire cathode surface hydrophilia when using a travelling wire in wire electrochemical micro machining". *Journal of Materials Processing Technology*, 2016. 235: 68-74.
11. N.S. Qu, K. Xu, Y.B. Zeng, and Qia Yu, "Enhancement of the Homogeneity of Micro Slits Prepared by Wire Electrochemical Micromachining". *Int. J. Electrochem. Sci.*, 2013. 8: 12163-12171.
12. K. Xu, Y.B. Zeng, P. Li, X.L. Fang, and D. Zhu, "Experimental Research on Multiple Wire Electrode Electrochemical Micro Machining". *Int. J. Electrochem. Sci.*, 2016. 11: 5403-5415.
13. Wang Xiangyang, Fang Xiaolong, Zeng Yongbin, and Qu Ningsong, "Fabrication of Micro Annular Grooves on a Cylindrical Surface in Aluminum Alloys by Wire Electrochemical Micromachining". *Int. J. Electrochem. Sci.*, 2016. 11: 7216-7229.
14. Fang Xiaolong, Zou Xianghe, Zhang Pengfei, Zeng Yongbin, and Qu Ningsong, "Improving machining accuracy in wire electrochemical micromachining using a rotary helical electrode". *Int J Adv Manuf Technol*, 2016. 84: 929-939.
15. Zou Xianghe, Fang Xiaolong, Zeng Yongbin, Zhang Pengfei, and Zhu Di, "In Situ Fabrication of Ribbed Wire Electrodes for Wire Electrochemical Micromachining". *Int. J. Electrochem. Sci.*, 2016. 11: 2335-2344.
16. Haidong He, Ningsong Qu, Yongbin Zeng, Xiaolong Fang, and Yangyang Yao "Machining accuracy in pulsed wire electrochemical machining of γ -TiAl alloy". *Int J Adv Manuf Technol*, 2016. DOI: 10.1007/s00170-016-8402-1.

17. Fang Xiaolong, Li Peng, Zeng Yongbin, and Zhu Di, "Research on Multiple Wires Electrochemical Micromachining with Ultra-short Voltage Pulses". *Procedia CIRP*, 2016. 42: 423-427.
18. D. Zhu, K. Wang, and N. S. Qu, "Micro Wire Electrochemical Cutting by Using In Situ Fabricated Wire Electrode". *Annals of the CIRP*, 2007. 56(1): 241-244.
19. Shaohua Wang, Yongbin Zeng, Yong Liu, and Di Zhu "Micro wire electrochemical machining with an axial electrolyte flow". *Int J Adv Manuf Technol*. 2011. DOI: 10.1007/s00170-011-3858-5.
20. Vladimir M. Volgin, Van Dong Do, and Alexey D. Davydov, "Modeling of wire electrochemical machining". *Chemical Engineering Transactions*, 2014. 41: 91-96.